




Endothelial basement membrane laminin 511 is essential for shear stress response

Jacopo Di Russo^{1,2} , Anna-Liisa Luik^{1,2} , Lema Yousif^{1,2}, Sigmund Budny^{1,2}, Hans Oberleithner^{2,3}, Verena Hofschroer^{2,3}, Juergen Klingauf^{2,4}, Ed van Bavel⁵, Erik NTP Bakker⁵, Per Hellstrand⁶, Anirban Bhattachariya⁶, Sebastian Albinsson⁶, Frederic Pincet^{7,8}, Rupert Hallmann^{1,2} & Lydia M Sorokin^{1,2,*} 

Abstract

Shear detection and mechanotransduction by arterial endothelium requires junctional complexes containing PECAM-1 and VE-cadherin, as well as firm anchorage to the underlying basement membrane. While considerable information is available for junctional complexes in these processes, gained largely from *in vitro* studies, little is known about the contribution of the endothelial basement membrane. Using resistance artery explants, we show that the integral endothelial basement membrane component, laminin 511 (laminin $\alpha 5$), is central to shear detection and mechanotransduction and its elimination at this site results in ablation of dilation in response to increased shear stress. Loss of endothelial laminin 511 correlates with reduced cortical stiffness of arterial endothelium *in vivo*, smaller integrin $\beta 1$ -positive/vinculin-positive focal adhesions, and reduced junctional association of actin–myosin II. *In vitro* assays reveal that $\beta 1$ integrin-mediated interaction with laminin 511 results in high strengths of adhesion, which promotes p120 catenin association with VE-cadherin, stabilizing it at cell junctions and increasing cell–cell adhesion strength. This highlights the importance of endothelial laminin 511 in shear response in the physiologically relevant context of resistance arteries.

Keywords endothelial cells; focal adhesions; laminin 511; shear stress; VE-cadherin

Subject Categories Cell Adhesion, Polarity & Cytoskeleton; Vascular Biology & Angiogenesis

DOI 10.15252/embj.201694756 | Received 11 May 2016 | Revised 8 November 2016 | Accepted 9 November 2016 | Published online 9 December 2016

The EMBO Journal (2017) 36: 183–201

Introduction

The endothelium bound to its underlying basement membrane forms the inner seal of blood vessels and functions both as a selective barrier to soluble molecules and cells, and as a physiological sensor of changes in flow within the vessel lumen. Even small changes in shear and pressure are rapidly signalled to the underlying smooth muscle layers of the vessel wall, resulting in dilation or contraction of the vessel and thereby maintenance of constant flow and pressure. This occurs at the level of resistance arteries; 100- to 250- μ m-diameter vessels that form the large body of the vascular bed and therefore play a central role in vascular homeostasis.

The detection of changes in shear stress requires a junctional complex containing PECAM-1, VE-cadherin and VEGF receptor 2 (VEGFR2) and VEGFR3, as well as anchorage to the extracellular matrix (ECM) as demonstrated by a dependency on $\beta 1$ - and $\beta 3$ -integrins (Davies *et al*, 1994; Orr *et al*, 2006). Considerable data suggest that increased force/shear stress on PECAM-1 leads to Src kinase activation (Chiu *et al*, 2008) and phosphorylation and ligand independent activation of VEGFR2 and VEGFR3. Activated VEGFR2 and VEGFR3 can trigger several pathways that lead to the activation of integrins and subsequent downstream signalling, including the release of vasoactive signals and vessel dilation (Jin *et al*, 2003; Fleming *et al*, 2005). Shear detection requires cell anchorage to the underlying ECM, the nature of which appears to influence the response of the endothelium, since endothelial cells bound to fibronectin versus collagen type I lead to stronger adhesion, manifested as larger and more complex focal adhesions and stronger tension development on PECAM-1 (Collins *et al*, 2014).

In contrast to PECAM-1, tension across VE-cadherin does not increase under flow but VE-cadherin is nevertheless essential for shear response (Conway *et al*, 2013). The role of VE-cadherin is not

1 Institute of Physiological Chemistry and Pathobiochemistry, University of Muenster, Muenster, Germany

2 Cells-in-Motion Cluster of Excellence, University of Muenster, Muenster, Germany

3 Institute of Physiology II, University of Muenster, Muenster, Germany

4 Institute of Medical Physics, University of Muenster, Muenster, Germany

5 Biomedical Engineering and Physics, Academic Medical Centre, University of Amsterdam, Amsterdam, The Netherlands

6 Department of Experimental Medical Science, Lund University, Lund, Sweden

7 Laboratoire de Physique Statistique, École Normale Supérieure – PSL Research University, Paris, France

8 CNRS UMR8550, Sorbonne Universités – UPMC Univ Paris 06, Université Paris, Paris, France

*Corresponding author. Tel: +49 251 8355581; Fax: +49 251 83 55596; E-mail: sorokin@uni-muenster.de

clear but it most likely regulates the strength of adhesion between individual cells (Daneshjou *et al*, 2015). In addition, it has been recently shown to interact with VEGFR2 and VEGFR3 and Src kinases, which was hypothesized to facilitate phosphorylation of VEGFR2 and VEGFR3 (Coon *et al*, 2015) and thereby promote downstream signalling events.

Stable endothelial cell–cell junctions via VE-cadherin-mediated interactions are required for normal vascular homeostasis and are remodelled in cases of inflammation but also physiological processes, such as angiogenesis. Recent data have shown enhanced displacement of VE-cadherin from junctions to internal vesicles in a $\beta 1$ -integrin-dependent manner during angiogenic events in the mouse retina (Yamamoto *et al*, 2015). As $\beta 1$ -integrins bind mainly ECM ligands, this suggests that the endothelial ECM may also affect junctional tightness. We, therefore, here address whether endogenous endothelial basement membrane components of resistance arteries can affect physiological processes required for blood flow and pressure regulation.

Data on ECM and shear detection stem mainly from *in vitro* models using fibronectin and collagen type I as substrates that are relevant to pathological situations, such as atherosclerosis, but do not occur in the endothelial basement membrane of healthy, mature arterioles. Both fibronectin and collagen type I occur predominantly in the interstitial matrix of the arteriole wall, which underlies the endothelial basement membrane, and are not in direct contact with endothelial cells, unless the luminal layer is damaged or the vessel is fibrotic. Rather, the endothelium of healthy resistance arteries is anchored to the basement membrane, which consists of collagen type IV, laminins, nidogens and heparan sulphate proteoglycans, all of which are large families of proteins containing several members that can assemble differentially to form biochemically and functionally distinct basement membranes. Of all these components, the laminins are considered to convey biological activity and to account for the functional differences between basement membranes. In the endothelial cell basement membrane, laminin $\alpha 4$ and $\alpha 5$ chains occur bound to $\beta 1$ and $\gamma 1$ chains to form laminins 411 and 511. Laminin 411 is ubiquitously expressed in all endothelial basement membranes from the first stages of tube formation (Hallmann *et al*, 2005) and has been shown to play a role in angiogenesis in some tissues (Stenzel *et al*, 2011). By contrast, laminin $\alpha 5$ first appears surrounding arteries when the heart commences to beat (E10) and when blood pressure is initiated, and only much later in basement membranes of microvessels (Sorokin *et al*, 1997); it has been implicated in immune cell extravasation (Sixt *et al*, 2001a; Wu *et al*, 2009). Both laminin isoforms have been reported to interact with $\beta 1$ -integrins (Kikkawa *et al*, 2000; Nielsen & Yamada, 2001; Sixt *et al*, 2001b) and laminin 511 also with the RGD-binding integrins (Sasaki & Timpl, 2001). Whether these endothelial laminins also affect cell–cell adhesion and play a role in vascular homeostasis has not been previously addressed.

We here employ resistance arteries from the mesenterium of mice lacking laminin $\alpha 4$ or $\alpha 5$ in endothelial basement membranes in *ex vivo* shear and pressure experiments, revealing almost complete absence of a shear response in vessels lacking laminin $\alpha 5$. *In vitro* and *in vivo* analyses suggest that $\beta 1$ -integrins mediate endothelial binding to the laminin $\alpha 5$ chain, which stabilizes VE-cadherin at the adherens junctions, thereby enhancing the strength

of cell–cell adhesion. This demonstrates the importance of the endothelial basement membrane in shear detection by resistance arteries and hence vascular homeostasis.

Results

Laminin 511 is required for resistance artery shear stress response

To investigate whether the endothelial laminins affected the response of resistance arteries to changes in shear force within vessel lumens, resistance arteries dissected from the mesenterium of *Tek-Cre::Lama5^{-/-}* and *Lama4^{-/-}* mice were employed in *ex vivo* experiments. Varying the shear stress in isolated resistance arteries from wild-type mice (WT) resulted in a dilatatory response that ranged from 10 μm at 2.5 dyn/cm² to 30 μm at 40 dyn/cm². The same experiment performed using *Tek-Cre::Lama5^{-/-}* arteries revealed almost complete lack of dilation, while *Lama4^{-/-}* arteries showed a significantly enhanced dilatatory response (Fig 1A and Appendix Fig S1A and B).

To respond to changes in shear stress, not only proper attachment of the endothelium to the basement membrane is essential but also the capacity of the endothelium to generate vasodilatory substances. In turn, smooth muscle cells need to be able to respond to both dilatatory and contractile stimuli. We therefore tested response to a muscarinic receptor agonist, methacholine, and to the thromboxane A2 receptor agonist, U46619, using a wire myograph set-up. Methacholine induces the release of dilatatory substances from the endothelium, including NO, while U46619 directly induces vasoconstriction. Dose responses to these two factors were indistinguishable between WT, *Lama4^{-/-}* and *Tek-Cre::Lama5^{-/-}* resistance arteries (Fig 1B and C, and Appendix Fig S1C and D), indicating absence of compromised endothelial or smooth muscle function in either of the KO mice. To further test for defects in smooth muscle function, dose responses to sodium nitroprusside (SNP), a nitric oxide donor, and phenylephrine, an $\alpha 1$ adrenergic receptor agonist, were tested in WT, *Lama4^{-/-}* *Tek-Cre::Lama5^{-/-}* resistance arteries, revealing no differences (Appendix Fig S1C and D). Taken together, these data suggest that the impaired shear stress response in the *Lama4^{-/-}* and *Tek-Cre::Lama5^{-/-}* resistance arteries originates from an autonomous endothelial cell defect in response to mechanical stress.

Morphological analyses of the KO mice revealed the absence of fibrosis or other changes in ECM expression in the endothelial layer or the smooth muscle layers of the mesenteric artery wall, which could indirectly affect shear stress response by changing the stiffness of the vessel. Laminin $\alpha 5$ was absent from all endothelial cell basement membranes in *Tek-Cre::Lama5^{-/-}* (Fig 2A and Appendix Fig S2A) and laminin $\alpha 4$ was not detectable in both endothelial and smooth muscle basement membranes in *Lama4^{-/-}* mice, as revealed by 3D confocal microscopy of whole-mount-stained mesenteric resistance arteries (Fig 2A). Only larger vessels in *Tek-Cre::Lama5^{-/-}* mice showed laminin $\alpha 5$ reactivity in association with perivascular cells and smooth muscle basement membranes. Scanning EM of mesenteric arteries denuded of endothelium (Fig 2B) revealed the absence of differences from WT vessels in basement membrane topography or integrity in both KO

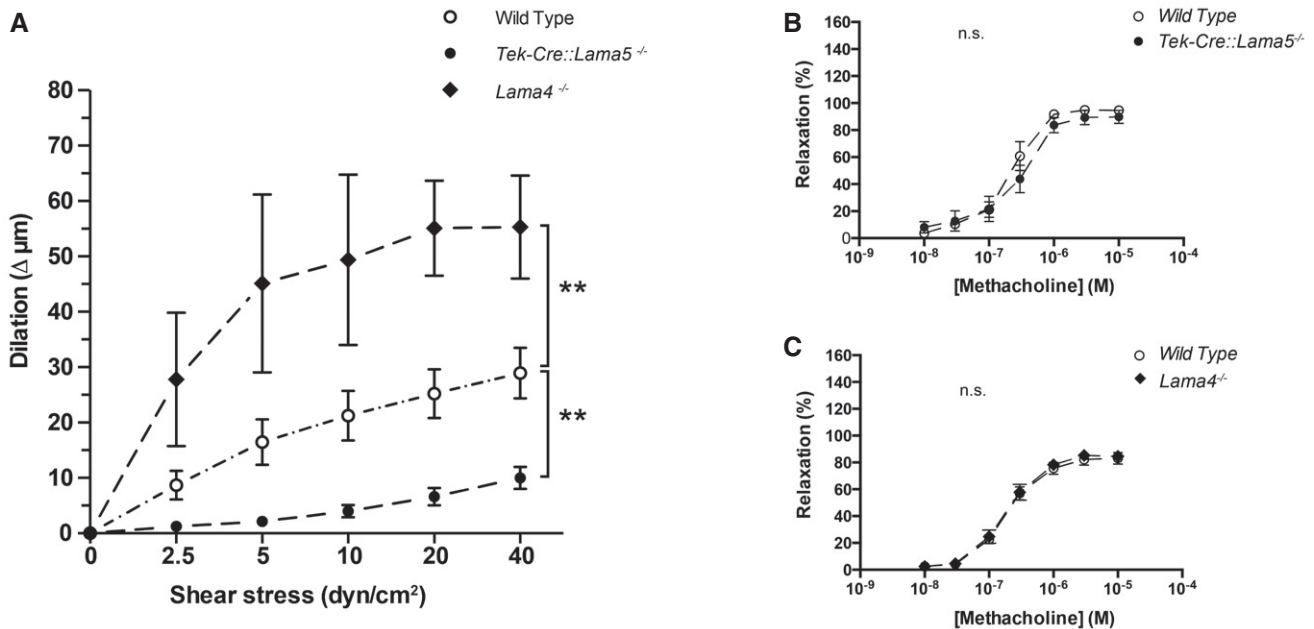


Figure 1. Impaired endothelial cell-mediated response to shear stress in laminin KO mice.

- A Shear-dilation relations of *Tek-Cre::Lama5^{-/-}* and *Lama4^{-/-}* mesenteric resistance arteries and corresponding wild-type controls show a reduced response of *Tek-Cre::Lama5^{-/-}* arteries and an enhanced response of *Lama4^{-/-}* arteries. Data shown are mean changes in vessel diameter ($\Delta \mu\text{m}$) \pm s.e.m. from eight experiments with 16 wild-type and 16 KO arteries; KO and wild type were analysed as pairs in each experiment. ****** $P < 0.01$, paired *t*-test.
- B, C The dose-response curves of arteries from wild-type, *Tek-Cre::Lama5^{-/-}* (B) and *Lama4^{-/-}* mice (C) and wild-type littermates stimulated with methacholine do not show significant differences (n.s.). Data are expressed as per cent relaxation of the maximum force developed in the presence of 0.3 μM U46619 and are mean values \pm s.e.m. from seven experiments with one wild-type artery and one KO artery in each experiment.

strains (Fig 2B). Immunofluorescence staining for basement membrane components and interstitial matrix molecules, including fibronectin and collagen type I, showed no differences between WT, *Lama4^{-/-}* and *Tek-Cre::Lama5^{-/-}* arteries in staining intensities or patterns for any of the molecules tested (Fig 2 and Appendix Fig S2B, Table 1). Only *Lama4^{-/-}* mice, which have been previously characterized (Thyboll *et al*, 2002), show an aberrant ubiquitous expression of laminin $\alpha 5$ in all endothelial basement membranes (Wu *et al*, 2009).

The observed defects in shear response, therefore, stem from the loss of laminin $\alpha 5$ or laminin $\alpha 4$ or, in the case of *Lama4^{-/-}* mice, a ubiquitous and more even expression of laminin $\alpha 5$, and not indirect effects due to compensatory expression of other ECM molecules.

Loss of laminin 511 results in inward remodelling of resistance arteries to maintain blood pressure constant

Given the dramatic changes in shear response in the absence of the endothelial laminins, we examined whether mean systolic and diastolic blood pressure were altered in *Lama4^{-/-}* and *Tek-Cre::Lama5^{-/-}* mice using intra-carotid artery measurements. Appendix Fig S3 shows that there were no significant differences from WT littermates in both strains. In addition, we investigated morphological changes known to correlate with chronic alterations in shear, revealing that *Tek-Cre::Lama5^{-/-}* resistance arteries, which show almost no shear detection, have reduced vessel diameters, while *Lama4^{-/-}* resistance arteries, which showed a more

Figure 2. Laminin composition of laminin KO resistance arteries and topography of the endothelial basement membranes.

- A Three-dimensional digital reconstructions of optical sections through immunofluorescently stained mesenteric resistance arteries from wild-type, *Tek-Cre::Lama5^{-/-}* and *Lama4^{-/-}* mice, and optical sections through vessel walls to show the endothelial and underlying smooth muscle layers. DAPI staining permits identification of endothelial cell nuclei, which lie perpendicular to the nuclei of the smooth muscle cells. Laminin $\alpha 5$ is absent from endothelial basement membranes of *Tek-Cre::Lama5^{-/-}* arteries (arrow) but is still present in smooth muscle basement membranes (asterisk), while laminin $\alpha 4$ is still detectable in both endothelial and smooth muscle basement membranes. *Lama4^{-/-}* arteries lack laminin $\alpha 4$ in both endothelial (arrow) and smooth muscle (asterisk) basement membranes, but laminin $\alpha 5$ is still detectable. Scale bars are 10 μm .
- B Scanning electron microscopy images of endothelial cell-denuded mesenteric resistance arteries show a comparable topography of the endothelial basement membrane in wild-type, *Tek-Cre::Lama5^{-/-}* and *Lama4^{-/-}* arteries. The arrows indicate artificial ruptures due to preparation procedure. Scale bars are 100 nm.
- C Intravital microscopic quantification of mesenteric arteries sizes *in vivo* shows smaller diameters (-24.3%) in *Tek-Cre::Lama5^{-/-}* arteries and larger diameters ($+27.6\%$) in *Lama4^{-/-}* arteries compared to wild-type controls. Autofluorescence of the internal elastic lamina allowed a good approximation of mesenteric arteries lumen diameter. Scale bar is 100 μm . Data are means \pm s.e.m. from a minimum of four first-order mesenteric arteries imaged at least in four mice per genotype. ***** $P < 0.05$ unpaired *t*-test.

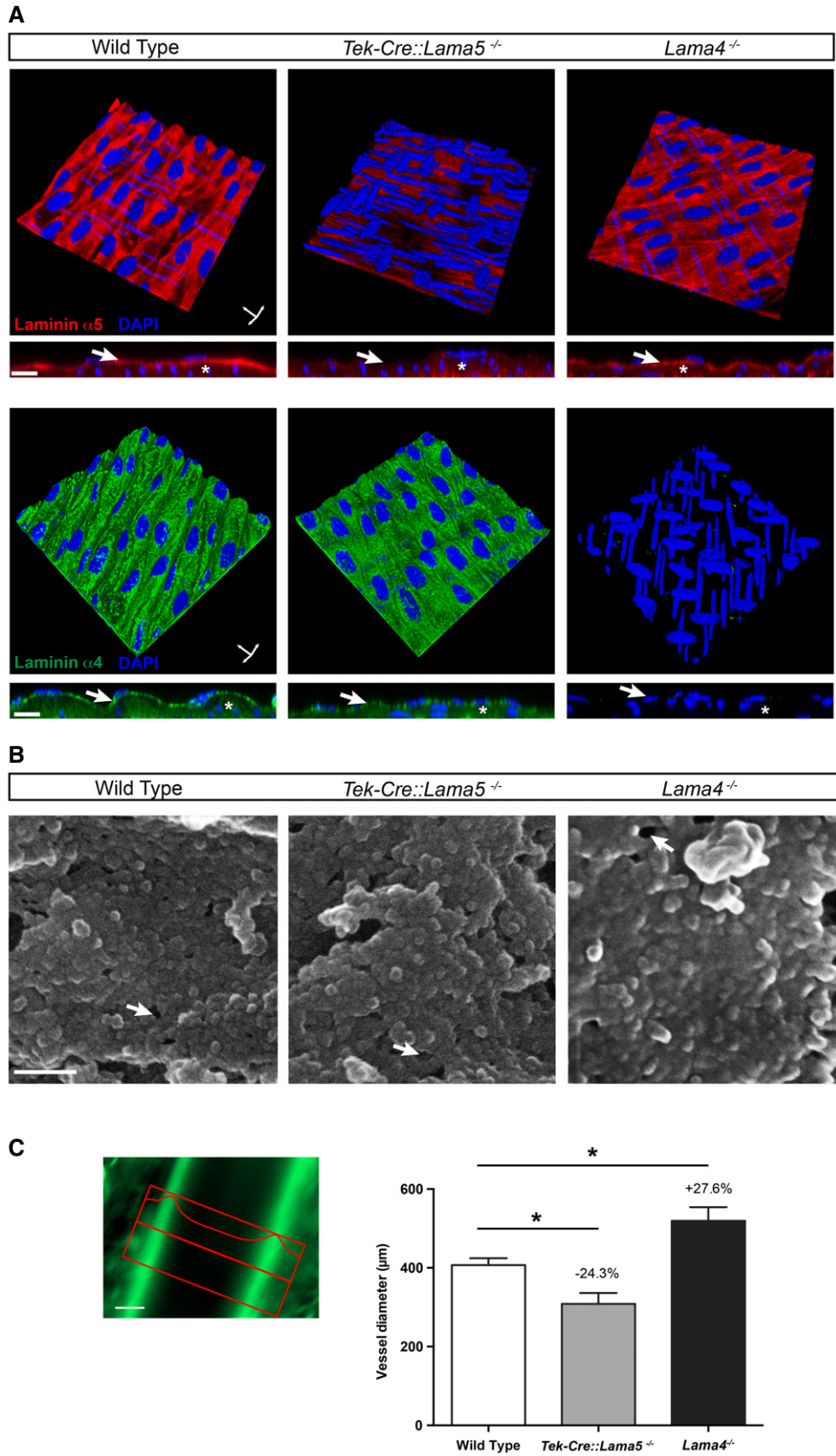


Figure 2.

Table 1. Overview of endothelial basement membrane and interstitial matrix components tested.

ECM protein	Wild type	<i>Tek-Cre::Lama5</i> ^{-/-}	<i>Lama4</i> ^{-/-}
Laminin $\alpha 1$	–	–	–
Laminin $\alpha 2$	–	–	–
Laminin $\alpha 3$	–	–	–
Laminin $\alpha 4$	+	+	–
Laminin $\alpha 5$	+	–	+*
Laminin $\beta 1$	+	+	+
Laminin $\beta 2$	+	+	+
Laminin $\gamma 1$	+	+	+
Laminin $\gamma 3$	–	–	–
Collagen type IV	+	+	+
Nidogen-1	+	+	+
Nidogen-2	+	+	+
Perlecan	+	+	+
Fibronectin	+	+	+
Collagen type I	+	+	+

+, present; –, not detectable; *, broader distribution.

sensitive response to shear, had larger vessel diameters (Fig 2C). This is consistent with inward vessel remodelling in *Tek-Cre::Lama5*^{-/-} and outward remodelling in *Lama4*^{-/-} in an effort to maintain blood pressure constant (Mulvany, 1999).

Laminin 511 interacts with integrin $\beta 1$ and influences focal adhesion size

To investigate whether arterial endothelial cells can bind equally well to both endothelial laminin isoforms, *in vitro* adhesion assays were performed using human umbilical artery endothelial cells (HUAECs). Control substrates included the non-endothelial laminin 111 and fibronectin. HUAECs showed dose-dependent and saturable binding to all substrates, albeit to different extents. Laminins 511 and 111 supported the highest degree of binding, and low levels of binding to laminin 411 were measured (Fig 3A), indicating preferential interaction with laminin 511 in the endothelial basement membrane. To define whether such interactions could induce release of endothelial cell-derived factors involved in shear-induced vasodilation, the prostacyclin secretion pathway was investigated in HUAECs plated at confluency onto purified laminin 511 versus laminin 111 and subjected to 10 dyn/cm² shear for 4 h or no shear.

It was not possible to use laminin 411 as the cells detached under even low flow conditions due to weak adhesion. Prostacyclin is released from endothelial cells under flow-induced shear (Frangos *et al*, 1985) and its expression is controlled by COX2 (Topper *et al*, 1996); hence, elevated COX2 expression reflects an enhanced shear response. Figure 3B shows a higher fold change in COX2 mRNA and protein expression in shear versus non-shear conditions in HUAECs plated on laminin 511 compared with laminin 111, consistent with a role for laminin 511 in shear-induced arterial dilation *in vivo*. In addition, endothelial cell alignment in the direction of flow, which provides an *in vitro* measure of shear responsiveness (Levesque & Nerem, 1985), revealed comparable rates of alignment of HUAECs plated on laminin 511 and fibronectin, but little or no alignment of cells plated on laminin 111 which remained perpendicular to flow (Fig 3C and Appendix Fig S4A).

Endothelial cells express several potential laminin 411 and 511 receptors (Kikkawa *et al*, 2000; Fujiwara *et al*, 2001; Sasaki & Timpl, 2001), some of which have been implicated in shear stress mechanotransduction processes (Jalali *et al*, 2001). To define which receptors mediate HUAEC binding to the endothelial laminins, functional-blocking antibodies to integrins $\beta 1$ (P5D2), $\alpha 3$ (P1B5), $\alpha 6$ (GoH3), $\alpha 5$ (P1D6) and αv (LM609) either alone or in combination were included in the adhesion assays. Fibronectin was employed as a positive control, where binding is known to be integrin $\alpha 5\beta 1$ -mediated (van der Flier *et al*, 2010). Laminin 111 was used as a non-endothelial laminin isoform. Adhesion assays revealed almost complete inhibition of HUAEC binding to laminins 511 and 411, laminin 111 and fibronectin by anti-integrin $\beta 1$ (Fig 3D and E), excluding the involvement of $\beta 3$ -integrins. This is consistent with the involvement of $\beta 1$ - but not $\beta 3$ -integrins in shear stress mechanotransduction (Jalali *et al*, 2001) and with the complete lack of integrin $\beta 3$ in endothelial cells of mesenteric arteries (Appendix Fig S4B). HUAEC binding to laminin 511 was predominantly integrin $\alpha 3$ -mediated, with strong synergistic effects of integrins $\alpha 3$ and $\alpha 6$ and to a less extent $\alpha 3$ and αv (Fig 3D). By contrast, binding to laminins 111 and 411 (Fig 3E) was mediated by integrin $\alpha 6\beta 1$ as shown by almost complete inhibition of binding by the GoH3 antibody, consistent with previous studies (Fujiwara *et al*, 2001). To test for potential species differences, similar experiments were performed with a skin-derived mouse endothelial cell line (sEND.1; Williams *et al*, 1989) revealing similar patterns of results as obtained with HUAECs (Appendix Fig S5A).

$\beta 1$ -Integrin-containing focal adhesions (FAs) have been shown to be important for shear stress mechanotransduction (Davies *et al*, 1994; Tzima *et al*, 2001), and changes in their size and number are regulated in response to the intensity of the mechanical load,

Figure 3. Arterial endothelial cells preferentially adhere to laminin 511 via $\beta 1$ -integrins.

- A *In vitro* cell adhesion assays employing HUAECs plated on increasing concentrations of purified laminin 411 and 511, compared to the non-endothelial cell laminin 111 and fibronectin, showing high levels of HUAEC adhesion to laminin 511 and low binding to laminin 411. Data are means \pm s.e.m. of 3 independent experiments with triplicates/experiment.
- B Enhanced fold change (Δ) in *Cox2* mRNA expression and protein levels in HUAECs plated on laminin 511 versus laminin 111 in response to shear. mRNA data are means \pm s.e.m. of four independent experiments with triplicates/experiment, paired *t*-test. Protein quantification data are means \pm s.e.m. of seven independent experiments, Mann–Whitney *U*-test. **P* < 0.05, ***P* < 0.01.
- C Angle histogram of HUAEC orientation after 120 min of 10 dyn/cm² shear stress showing the per cent cells at 10–90° in relation to the direction of flow. Cells were plated on 25 nM laminin 511 and laminin 111. Data are means \pm s.e.m. of six independent experiments, *t*-test. **P* < 0.05.
- D, E Inhibition assays performed at 25 nM laminin 511 (D), laminin 111, laminin 411 or fibronectin (E) in the presence or absence of function-blocking integrin antibodies. Data are means \pm s.e.m. of four experiments with triplicates/experiment, unpaired *t*-test. **P* < 0.05, ***P* < 0.01, ****P* < 0.001, *****P* < 0.0001.

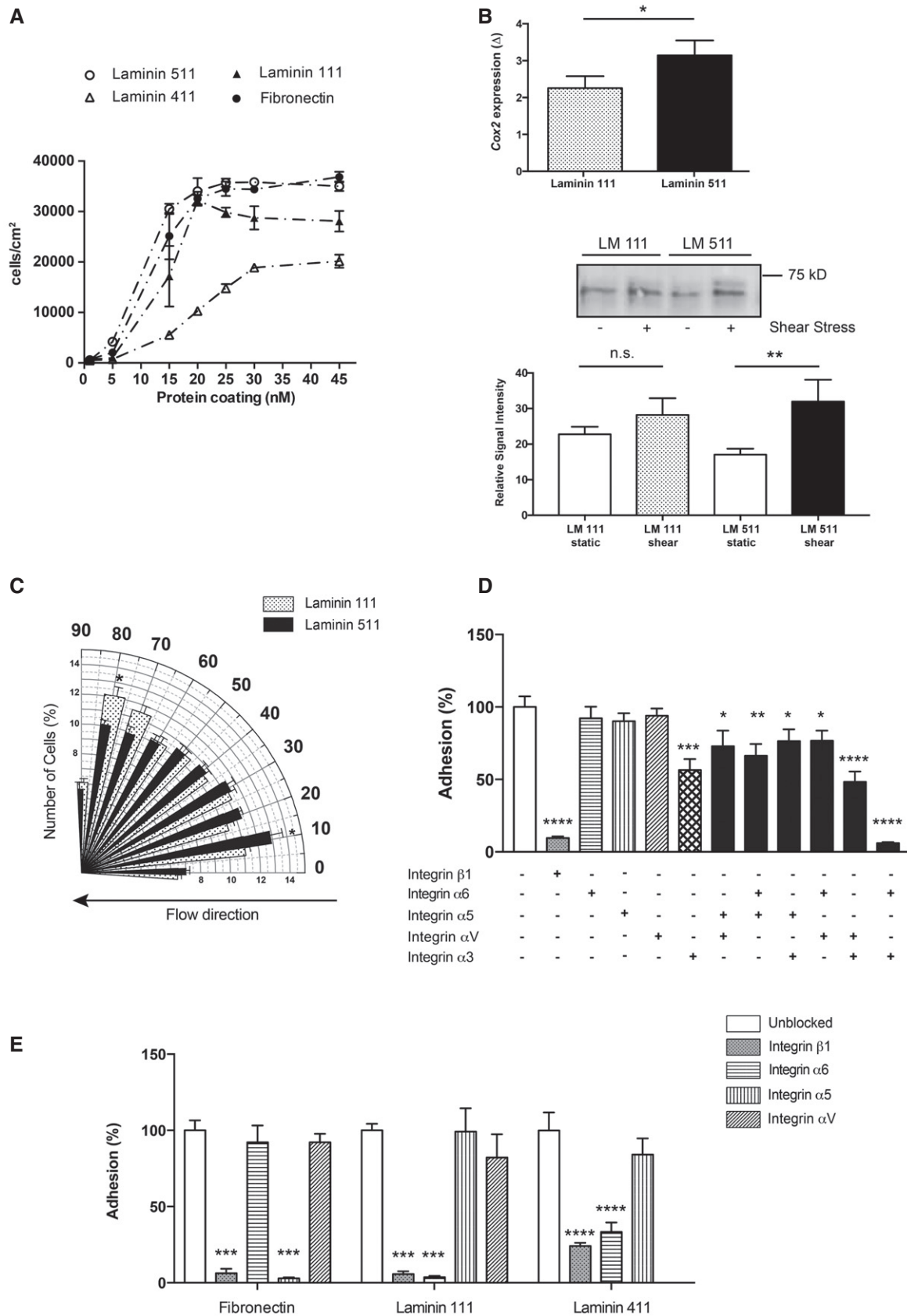


Figure 3.

thereby controlling the strength of adhesion (Jalali *et al*, 2001). However, few studies have examined FA *in vivo* (van Geemen *et al*, 2014). To investigate whether $\beta 1$ -integrin-containing FAs occur in the endothelium of resistance arteries and whether they change in the laminin knockout mice, *en face* staining of the endothelium in mesenteric resistance arteries for $\beta 1$ -integrin together with vinculin as a marker of adhesion complexes (Collins *et al*, 2014; van Geemen *et al*, 2014) was performed, revealing localization of integrin $\beta 1$ in adhesion complexes in the endothelium of WT, *Lama4*^{-/-} and *Tek-Cre::Lama5*^{-/-} mice (Fig 4A). Quantification of the number and size of the vinculin-positive adhesion complexes in the WT, *Lama4*^{-/-} and *Tek-Cre::Lama5*^{-/-} mesenteric resistance arteries revealed significantly smaller but more numerous adhesion complexes in the *Tek-Cre::Lama5*^{-/-} endothelium compared to WT littermates (Fig 4B–D). By contrast, a higher number of large adhesion complexes occurred in *Lama4*^{-/-} endothelium, which show ubiquitous laminin 511 expression in all endothelial basement membranes (Fig 4B–D and Appendix Fig S5B).

To directly test whether the endothelial laminins affect FA size and density, HUAECs were plated at confluent densities on laminins 511, 411 or 111 and stained for vinculin, confirming larger FAs in cells plated on laminin 511 than on laminin 411 or 111, with comparable density on laminin 511 and 411, but significantly lower density on the non-endothelial laminin 111 (Appendix Fig S5C). Since strength of adhesion has been correlated to FA size (Riveline *et al*, 2001), taken together these data suggest that integrin $\beta 1$ -mediated binding to laminin 511 supports stronger endothelial cell anchorage to the underlying basement membrane in resistance arteries than laminin 411.

Endothelial cell adhesion to laminin 511 increases cortical actin stiffness and junctional tension

As mechanotransduction requires the cytoskeleton to connect and transmit tensional forces from different regions of the cell (Geiger *et al*, 2009; Hahn & Schwartz, 2009), the cortical stiffness of endothelial cells in *Tek-Cre::Lama5*^{-/-}, *Lama4*^{-/-} and WT mice was measured using *ex vivo* arterial preparations and atomic force microscopy (AFM). Test experiments performed on mesenteric resistance arteries versus aortae revealed the absence of differences in endothelial cortical stiffness between the two vessel types (Appendix Fig S6A). The analyses were therefore performed on the less fragile and more accessible aortae, showing a significant reduction in cortical stiffness in *Tek-Cre::Lama5*^{-/-} aortic endothelial cells compared with WT littermates (Fig 4E). By

contrast, the *Lama4*^{-/-} endothelium had a significantly increased cortical stiffness compared to WT controls (Fig 4F). To investigate whether the observed differences in cortical stiffness were due to the presence or absence of laminin $\alpha 5$ or laminin $\alpha 4$, similar measurements were performed using the mouse sEND.1, which binds to laminin 411 and 511 (Appendix Fig S6). As HUAECs show weak binding to laminin 411, it was not possible to employ them in these experiments. Control experiments were therefore performed with laminin 111. Interestingly, sEND.1 responded to increasing concentrations of laminin 511 (0–30 $\mu\text{g}/\text{ml}$), but not laminin 411, with increased cortical stiffness (Appendix Fig S6B). HUAEC cortical stiffness was also higher on laminin 511 than on the same concentration of laminin 111 (Fig 4G). These data suggest a direct effect of laminin $\alpha 5$ on cortical stiffness of the resistance artery endothelium and, hence, the actin cytoskeleton arrangement, which is also crucial for shear stress response (Hutcheson & Griffith, 1996).

As cortical actin dynamics and tension have been shown to control cadherin adhesion at adherens junctions (Engl *et al*, 2014) and VE-cadherin is required for shear stress sensing and mechanotransduction (Tzima *et al*, 2005), we investigated whether arterial endothelial cell binding to laminin 511 or 411 affects adherens junction tension using a dual pipette-pulling assay (Fig 5A). HUAECs were allowed to bind to laminin 411- or laminin 511-coated beads. Cells attached to beads were then permitted to bind to each other, and the strength required to detach two cells was measured (cell–cell adhesion strength). Previous studies have shown that adhesion complexes form in cells bound to the ECM-coated beads (Martinez-Rico *et al*, 2010). It was not possible to measure cell–cell adhesion strength after adhesion to laminin 411 due to the weak adhesion of HUAECs to this laminin isoform. Laminin 111 was therefore employed as a surrogate, as above in the AFM studies.

Cell–cell adhesion strength was significantly higher for HUAECs bound to laminin 511-coated beads compared to laminin 111-coated beads or single cells not bound to beads (Fig 5B). To test whether laminin 511 specifically affects adherens junctions, the same experiments were performed in the presence of functional-blocking antibody to the integral adherens junction molecule, VE-cadherin (BV9), revealing significantly reduced cell–cell adhesion strength (Fig 5C).

To test whether these effects were due to strength of laminin 511-induced adhesion or signalling events independent of adhesion strength, soluble laminin 511 was added to HUAECs alone (without beads) and cell–cell adhesion strength was measured. Interestingly, this revealed a similarly enhanced cell–cell adhesion strength as

Figure 4. Laminin 511 affects the size of endothelial adhesion complexes and cortical stiffness.

- A Double immunofluorescence staining of whole-mount wild-type mesenteric resistance arteries for $\beta 1$ integrin and vinculin shows colocalization in focal adhesions (arrowheads). Scale bar is 10 μm .
- B Vinculin immunofluorescence staining of whole-mount wild-type, *Tek-Cre::Lama5*^{-/-} and *Lama4*^{-/-} mice mesenteric resistance arteries reveals smaller adhesion complexes in *Tek-Cre::Lama5*^{-/-} (arrowheads) and larger adhesion complexes in *Lama4*^{-/-} vessels (arrowheads). Scale bar is 10 μm .
- C, D Corresponding quantification of sizes (C) and frequency distribution (D) of adhesion complexes per endothelial cell. Data are means \pm s.e.m. from 300 cells from nine wild-type and nine KO arteries isolated from three mice/genotype. *** $P < 0.001$, **** $P < 0.0001$, unpaired t-test.
- E, F The endothelium of excised wild-type, *Tek-Cre::Lama5*^{-/-} and *Lama4*^{-/-} aortae was analysed by AFM, revealing reduced cortical stiffness in *Tek-Cre::Lama5*^{-/-} vessels (–9.5%) and increased cortical stiffness in *Lama4*^{-/-} vessels (+2%). Data are means \pm s.e.m. from four experiments employing four KO arteries and four wild-type controls in each experiment. * $P < 0.05$, **** $P < 0.0001$, unpaired t-test.
- G *In vitro* AFM measurements of cortical stiffness performed on HUAECs plated on 30 nM purified laminin 511 or 111 reveal increased cortical stiffness in cells on laminin 511. Data are mean \pm s.e.m. from three experiments with triplicates/experiments, * $P < 0.05$, unpaired t-test.

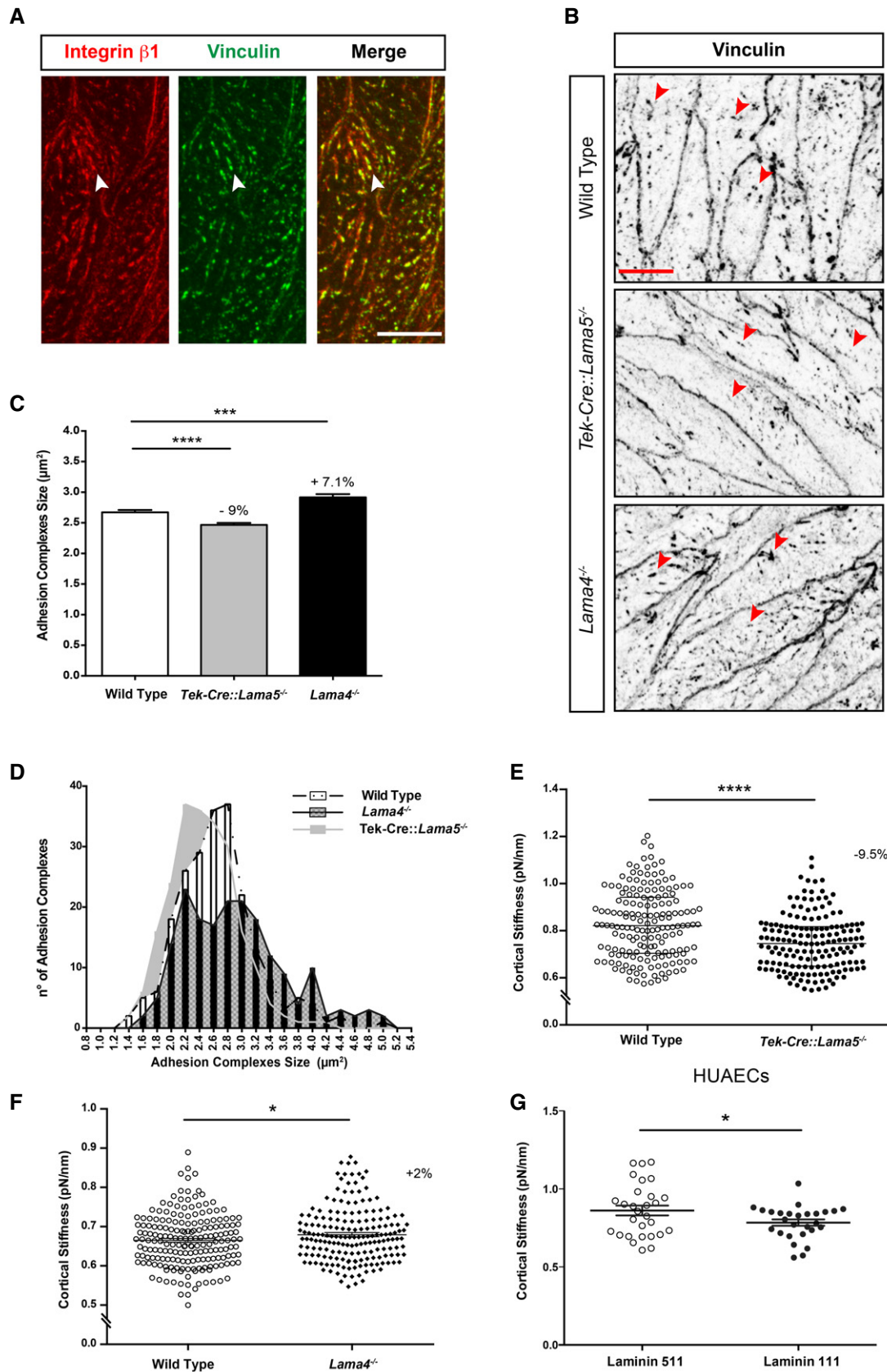


Figure 4.

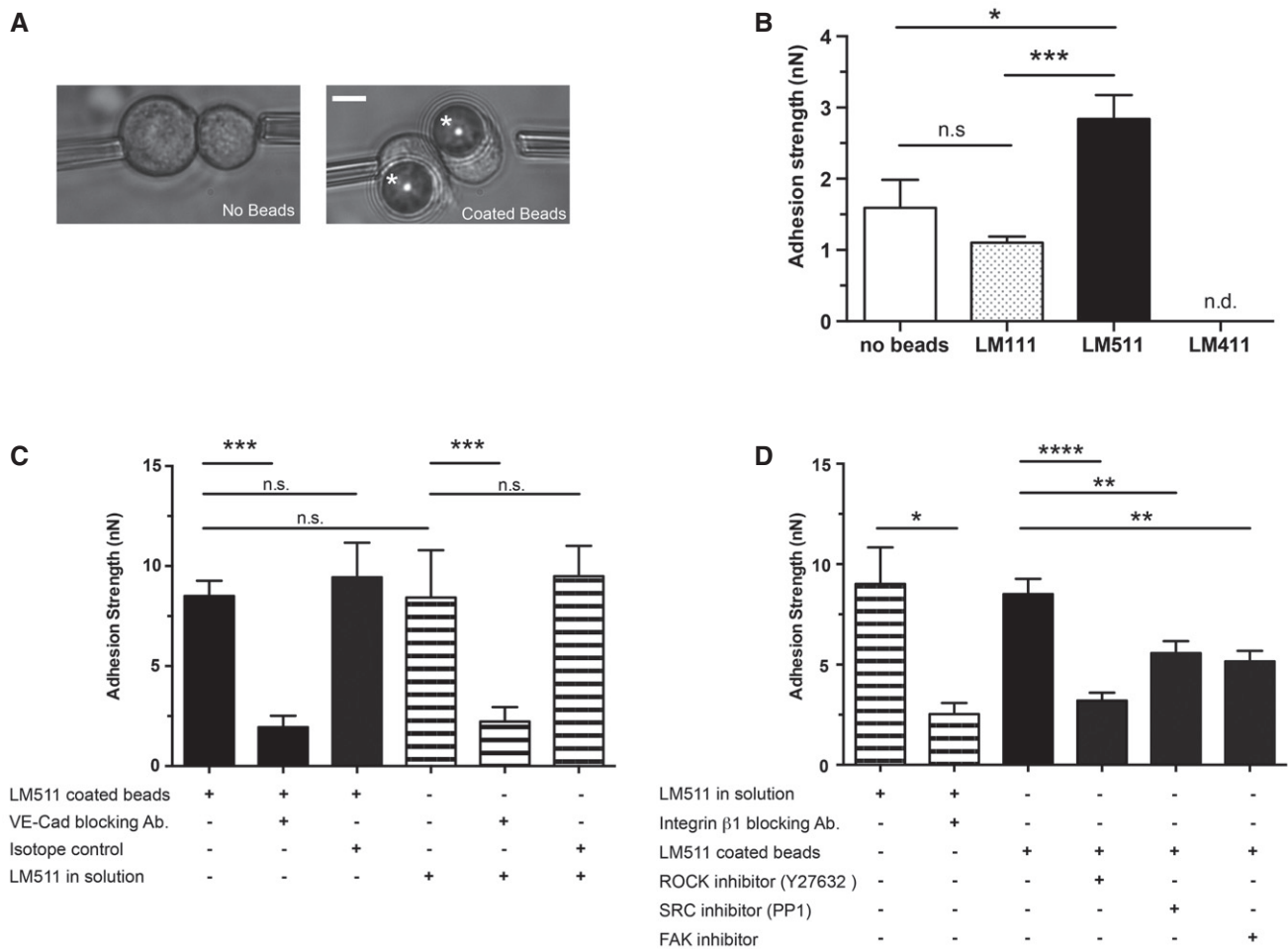


Figure 5. Laminin 511 increases cell–cell adhesion strength.

A A dual pipette-pulling assay was employed to measure cell–cell adhesion strength in HUAECs bound to laminin-coated beads (asterisk) or in the absence of beads. Scale bar is 10 μ m.

B Quantification shows higher adhesion strength between cells bound to laminin 511-coated beads compared to laminin 111-coated beads or cells not incubated with beads. Measurements could not be made with cells incubated with laminin 411-coated beads since it was impossible to find cell–bead complexes. Values are means \pm s.e.m. from 15 cells from three independent experiments, unpaired *t*-test with Welch's correction. **P* < 0.05, ****P* < 0.001.

C Dual pipette-pulling assay performed in the presence of VE-cadherin-blocking antibody, isotope control and soluble laminin 511, showing almost complete ablation of adhesion strength in the presence of the blocking antibody in all conditions. Similar adhesion strengths were measured between cells in the presence of soluble laminin 511 and cells bound to laminin 511-coated beads.

D Adhesion strength in the presence of soluble laminin 511 was significantly reduced in the presence of integrin $\beta 1$ -blocking antibody; cell–cell adhesion strength between cells bound to laminin 511 coated beads was significantly reduced in the presence of ROCK, SRC or FAK inhibitors.

Data information: (C, D) Values are means \pm s.e.m. from 11 cells from three independent experiments, unpaired *t*-test with Welch's correction. **P* < 0.05, ***P* < 0.01, ****P* < 0.001, *****P* < 0.0001, n.s. = not significant, n.d. = not determined.

measured between cells bound to laminin 511-coated beads, and was also inhibited by the addition of anti-VE-cadherin and anti-integrin $\beta 1$ (Fig 5C and D).

Inhibition of events downstream of $\beta 1$ -integrin binding to laminin 511, including inhibition of focal adhesion kinase and Src kinase (Martinez-Rico *et al*, 2010), also reduced the cell–cell adhesion strengths (Fig 5D). Similarly, inhibition of RhoA signalling, which has been implicated in both VE-cadherin junctional localization and can also occur downstream of laminin– $\beta 1$ integrin-mediated interactions (Yamamoto *et al*, 2015), significantly reduced cell–cell adhesion strengths (Fig 5D). Taken together, the data

suggest that the enhanced VE-cadherin-mediated cell–cell adhesion requires laminin 511 engagement with $\beta 1$ -integrin but that laminin 511 may also act as a signalling molecule independent of its strong adhesive effects.

Laminin $\alpha 5$ stabilizes VE-cadherin at the cell–cell junction

Cell–cell adhesion can be controlled by the complexity of junctional complexes or by the proportion of VE-cadherin molecules located at junctions versus those recycling (Yamamoto *et al*, 2015). HUAEC cells were therefore plated at confluent densities on laminin 511,

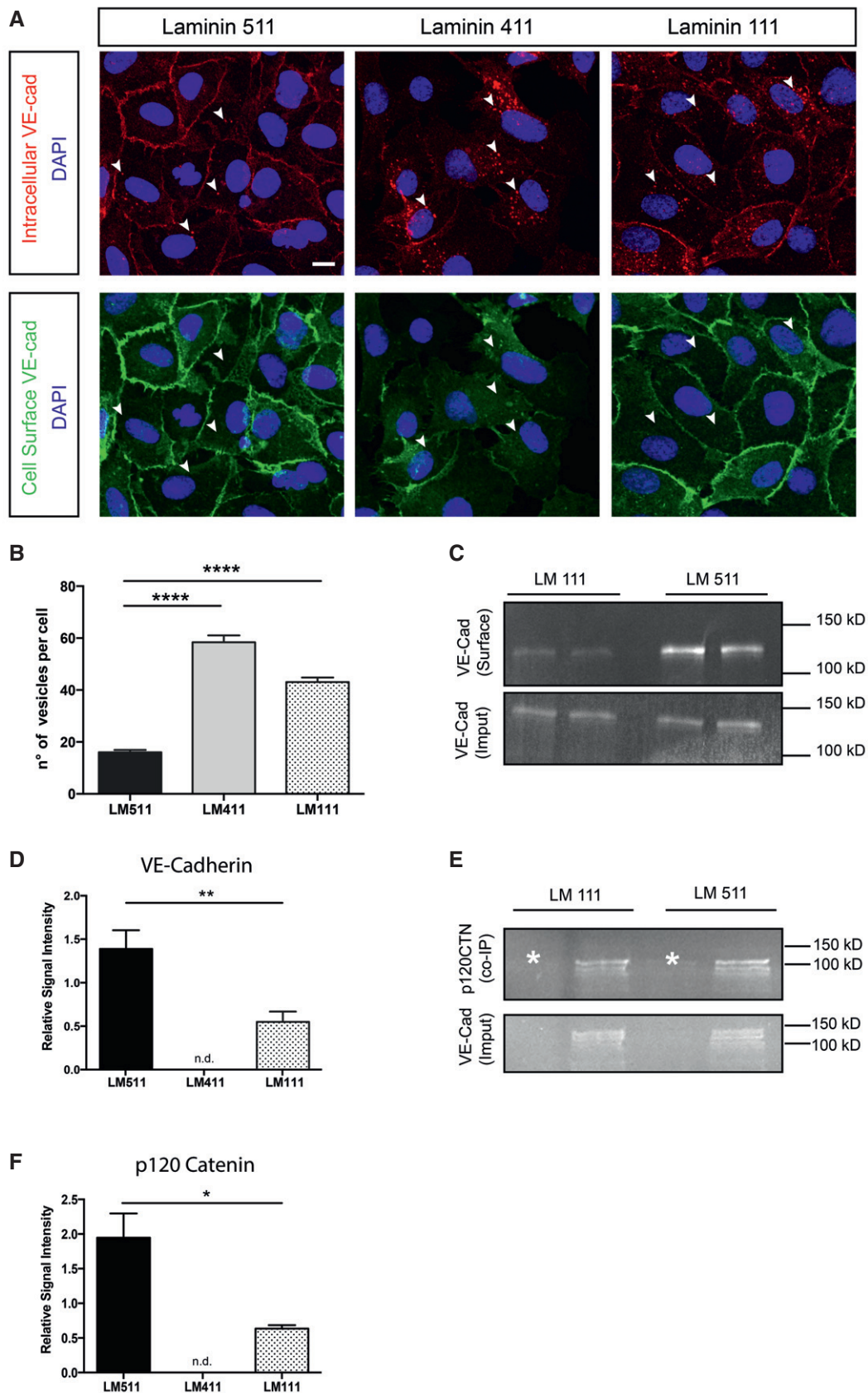


Figure 6.

Figure 6. Laminin 511 stabilizes VE-cadherin at cell–cell junctions.

- A Immunofluorescence-based antibody-feeding assay performed using HUAECs seeded on laminin 411-, 511- or 111-coated coverslips reveals more VE-cadherin at junctions and less in vesicles in cells plated on laminin 511 (arrowheads mark VE-cadherin-positive vesicles). Scale bar is 10 μ m.
- B Quantification of VE-cadherin-positive vesicles/cell in HUAECs plated on laminin 411, 511 or 111. Values are means \pm s.e.m. from 300 cells from three independent experiments, unpaired *t*-test. *****P* < 0.0001.
- C Western blot of biotinylated (surface) VE-cadherin in HUAECs plated on different laminins versus total VE-cadherin (input) confirms more junctionally located VE-cadherin in cells bound to laminin 511.
- D Quantification of Western blots expressed as relative signal proportions (surface VE-cadherin/total VE-cadherin). Values shown are means \pm s.e.m. of six experiments, unpaired *t*-test. ***P* < 0.01.
- E, F (E) Western blot of p120 catenin co-immunoprecipitated with VE-cadherin (input) from HUAECs plated on different laminins, and (F) corresponding quantification of the p120 signal intensity relative to the total VE-cadherin signal. Asterisks are isotope controls. Values shown are means \pm s.e.m. of four experiments, Mann–Whitney *U*-test. **P* < 0.05.

laminin 411 or laminin 111, and the VE-cadherin recycling rate was measured with an antibody-feeding assay (Yamamoto *et al*, 2015). Cells plated on laminin 511 showed lower proportions of vesicles containing internalized VE-cadherin after 30 min of antibody feeding compared to cells plated on laminin 411 or laminin 111 (Fig 6A and B). We confirmed that a higher fraction of VE-cadherin localized to the cell surface in cells plated on laminin 511 compared to laminin 111 by Western blot analysis of immunoprecipitated surface-biotinylated VE-cadherin compared to the total VE-cadherin content (Fig 6C and D). It was not possible to use laminin 411 due to the extreme low numbers of cells bound and hence difficulty in obtaining sufficient protein for Western blot analyses. Western blots of immunoprecipitated VE-cadherin for associated p120 catenin, which inhibits VE-cadherin endocytosis (Xiao *et al*, 2005; Chiasson *et al*, 2009), revealed higher levels of p120 catenin in HUAECs plated on laminin 511 compared to laminin 111 (Fig 6E and F).

The maintenance and stability of cell–cell junctions is regulated by the balance of cell–cell adhesion and cellular contractility (Liu *et al*, 2010; Yamamoto *et al*, 2015). We therefore compared the level of phosphorylated myosin light chain II (pMLC II) in WT, *Tek-Cre::Lama5^{-/-}* and *Lama4^{-/-}* mesenteric resistance arteries as a measure of actomyosin contractility (van Nieuw Amerongen *et al*, 2007; Abraham *et al*, 2009). As the number of endothelial cells that can be isolated from the mesenteric resistance arteries was insufficient for Western blot analyses, we investigated pMLC II (ser19) localization at cell–cell junctions by double immunofluorescence staining of whole-mount arteries for VE-cadherin and pMLC II and analysis by confocal microscopy. pMLC II staining in the proximity of the VE-cadherin-positive adherens junctions was most pronounced in *Lama4^{-/-}* mesenteric resistance arteries, with some junctional staining in WT arteries and the least observed in *Tek-Cre::Lama5^{-/-}* arteries (Fig 7A). To quantify this junction-associated pMLC II staining, we measured the length of continuous staining along the 3D adherens junction (Brevier *et al*, 2007), revealing significantly shorter stretches of junctional pMLC II in *Tek-Cre::Lama5^{-/-}* arteries, and longer stretches in *Lama4^{-/-}* arteries (Fig 7B). These data are consistent with enhanced stabilization of VE-cadherin at junctions in the *Lama4^{-/-}* mesenteric resistance arteries, which show ubiquitous laminin 511 expression. Given that junctional localization of VE-cadherin is also essential for efficient shear stress response (Tzima *et al*, 2005; Coon *et al*, 2015), it is also consistent with the almost complete lack of response to increased shear stress by mesenteric arteries lacking laminin $\alpha 5$.

Discussion

We show here that endothelial cell basement membrane laminin isoforms are required for a normal shear response by resistance arteries. The loss of laminin 511 from endothelial basement membranes in *Tek-Cre::Lama5^{-/-}* mice resulted in an almost complete ablation of dilation in response to increased shear stress, which correlated with reduced endothelial cell cortical stiffness and reduced size of integrin $\beta 1$ -positive/vinculin-positive focal adhesions. *In vitro* assays suggest that arterial endothelial cells directly bind to laminin 511 via $\beta 1$ integrins and that this interaction enhances VE-cadherin stabilization at cell–cell junctions, required for an adequate shear response (Fig 8).

The flow-induced defects observed in *Lama4^{-/-}* and *Tek-Cre::Lama5^{-/-}* resistance arteries were not due to defects in the ability of endothelial cells to communicate with the underlying smooth muscle cells, as demonstrated by comparable responses to methacholine, indicating the absence of endothelial cell intrinsic defects in the production of vasodilators. Nor were the smooth muscle cells compromised in their ability to contract or dilate in response to drugs or mechanical stimuli in either *Lama4^{-/-}* and *Tek-Cre::Lama5^{-/-}* resistance arteries, excluding the possibility that the observed defects in flow-induced dilation were due to smooth muscle cell malfunction. Importantly, the resistance arteries of the *Tek-Cre::Lama5^{-/-}* did not reveal any compensatory expression of other ECM molecules such as fibronectin, which has been previously shown to be required for shear detection and adhesion complex remodelling in *in vitro* studies. Only *Lama4^{-/-}* arteries showed an aberrant ubiquitous expression of laminin $\alpha 5$ throughout the endothelial cell basement membrane (Wu *et al*, 2009), and a hypersensitive response to shear. Our *in vivo* data therefore support a direct effect of laminin 511 on endothelial cell shear stress response. This was also supported by *in vitro* analyses showing enhanced COX2 expression and, thereby prostacyclin release, in HUAECs under shear when bound to laminin 511, as well as the alignment of HUAECs to the direction of flow when plated on laminin 511 but not on non-endothelial laminin 111.

Given the lower shear response in mice lacking endothelial laminin 511, one may have expected a higher blood pressure, which was not the case and was shown to be due to remodelling of the resistance arteries. Measures of vessel dimensions revealed a smaller lumen diameter in *Tek-Cre::Lama5^{-/-}* mice, while *Lama4^{-/-}* mice, which showed a hypersensitive response to shear, had larger diameter lumens, suggesting changes in the vessel wall to maintain blood pressure constant. Hence, while there was no

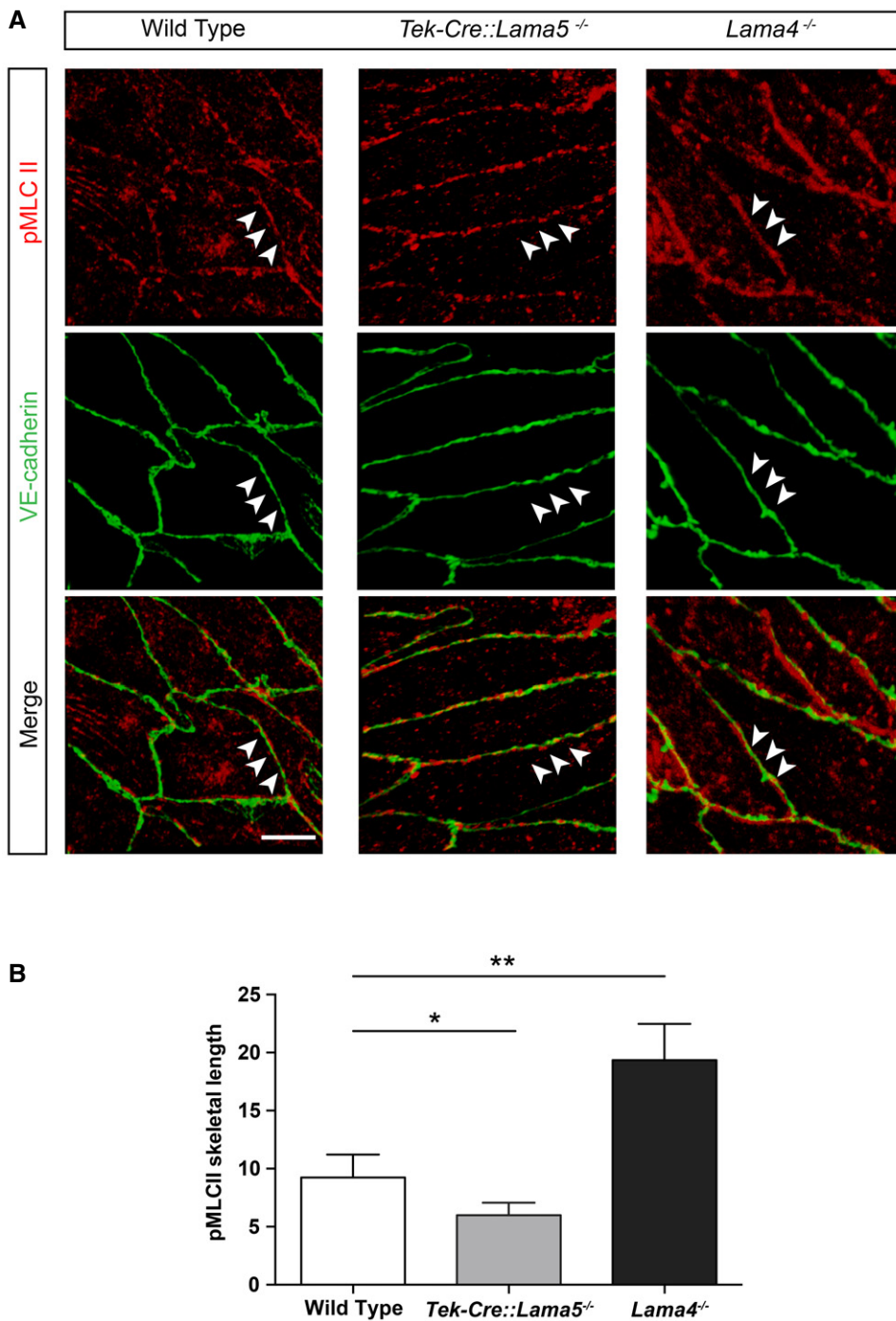


Figure 7. Laminin 511 affects the tension of endothelial cells adherens junctions *in vivo*.

A Double immunofluorescence staining for phosphorylated myosin light chain II (pMLC II) and VE-cadherin in mesenteric resistance artery endothelium from wild-type, *Tek-Cre::Lama5^{-/-}* and *Lama4^{-/-}* mice (arrowheads). Scale bar is 10 μ m.

B Quantification of the pMLC II signal along VE-cadherin signal revealed significantly less overlap in *Tek-Cre::Lama5^{-/-}* and more overlap in *Lama4^{-/-}* endothelium, compared with wild-type controls. The data are normalized to the skeletal length of the VE-cadherin signal. Values shown are means \pm s.e.m. resulting from quantification of four field of view per arteries, four mice/genotype. * $P < 0.05$, ** $P < 0.01$, paired t-test.

overt remodelling, such as increased collagen deposition and large changes in wall thickness (Mulvany, 1999), there were changes to the vessel dimensions to accommodate their inability to respond

appropriately to changes in flow, as reported in other mice models (Albinsson *et al*, 2007). There are reports of altered shear response in resistance arteries of diabetic and hypertensive rats (Matrougui

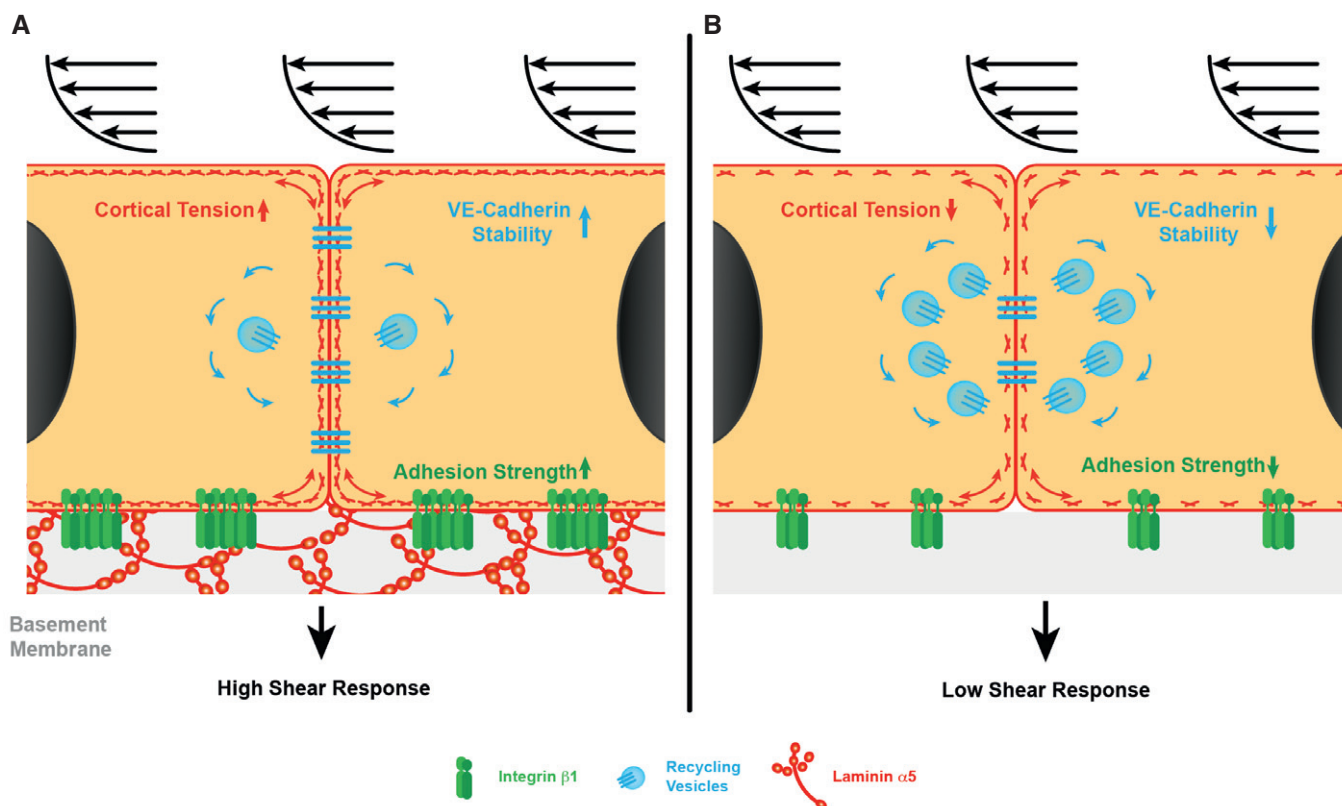


Figure 8. Central role of laminin $\alpha 5$ in shear response of resistance arteries.

- A Laminin $\alpha 5$ in the basement membrane supports strong adhesion of endothelial cells via $\beta 1$ integrins, which ensures the correct cortical tension and stabilizes VE-cadherin at cell-to-cell junctions, required for a normal shear response.
- B In the absence of laminin $\alpha 5$, the strength of endothelial cell adhesion is significantly reduced, leading to reduced cortical stiffness, less VE-cadherin at cell-to-cell junctions and correlated higher number of recycling VE-cadherin molecules, and a reduced shear response. Blue denotes recycling VE-cadherin-positive vesicles.

et al, 1998; Bouvet et al, 2007; Belin de Chantemele et al, 2009; Vessieres et al, 2012; Dumont et al, 2014) where expression or glycosylation state of extracellular matrix molecules is commonly affected (Intengan & Schiffrin, 2000; Rauch et al, 2011; Bogdani et al, 2014). However, there has been no investigation of whether changes in shear response in such pathological vessels are associated with changes in laminin isoform expression, a possibility that requires future investigation.

In vitro studies using HUVECs or BAEC plated onto fibronectin have shown that endothelial cells modulate the avidity and affinity of adhesion complexes upon increased shear stress, which results in increased adhesion strength and intracellular signalling (Urbich et al, 2000; Jalali et al, 2001; Tzima et al, 2001). This is consistent with the small adhesion complexes observed in the endothelium of *Tek-Cre::Lama5^{-/-}* arteries, which lack laminin 511 and have a reduced shear stress response, and the larger adhesion complexes in *Lama4^{-/-}* vessels, which express laminin 511 and have an enhanced response to shear stress. *In vitro* studies with HUAECs plated on laminin 511 versus laminins 411 or 111 supported the larger size and higher density of focal adhesions on laminin 511.

Our data suggest the involvement of $\beta 1$ - but not $\beta 3$ -integrins in arterial endothelial cell adhesion to laminin 511, consistent with published data (Kikkawa et al, 2000). In particular, integrin $\alpha 3\beta 1$

together with one or more other $\beta 1$ integrins appears to play a central role; however, conclusive identification of $\alpha 3\beta 1$ integrin *in vivo* is not possible at present, due to the absence of appropriate tools for use in mouse tissues. Our data suggest that the higher strength of adhesion provided by laminin 511 acts to stabilize VE-cadherin at cell-cell junctions by inhibiting its endocytosis, reflected in the enhanced association with p120 catenin (Xiao et al, 2005; Chiasson et al, 2009). This enhanced junctional localization of VE-cadherin induced by laminin 511 correlated with increased cell-cell adhesion strength as shown in the dual pipette-pulling assays and, *in vivo*, by the enhanced junctional phospho-myosin II staining in *Lama4^{-/-}* mice, which show an aberrant ubiquitous laminin $\alpha 5$ expression (van Nieuw Amerongen et al, 2007; Abraham et al, 2009). Others have shown that the strength of endothelial cell adhesion to the extracellular matrix affects the force that can be generated at junctions, across the force-sensing molecule PECAM-1 (Collins et al, 2014). Taken together, this suggests that one way in which laminin 511 in the endothelial cell basement membrane acts is to support greater strength of adhesion which permits greater force transduction across junctional force sensors and more sensitive shear response. In addition, the ability of soluble laminin 511 to enhance HUAEC cell-cell adhesion strength in the dual pipette experiments suggests a signalling role for laminin 511 independent

of its function as a strong adhesive substrate. Precisely how integrin $\beta 1$ -mediated endothelial interactions with laminin 511 act to stabilize VE-cadherin at junctions is not yet clear. However, data presented here suggest the involvement of both RhoA and Src kinases that are probably downstream of integrin-associated FAK events.

One possibility is that tissue/matrix stiffness directly affects the cytoskeleton and thereby cell behaviour (Discher *et al*, 2005; Halder *et al*, 2012), as described in the concept of cellular “tensegrity” (Ingber & Jamieson, 1985). Our work demonstrated that the presence of laminin $\alpha 5$ in endothelial basement membrane correlates with increased endothelial cell cortical stiffness *in vivo* and *in vitro*, which suggests changes in cortical actin arrangement may also mechanically affect junctional proteins (Engl *et al*, 2014; Sauteur *et al*, 2014). Although it is very difficult to prove, the absence of a single molecule such as laminin 511 from the basement membrane is unlikely to affect the overall stiffness of the matrix, plus the stiffness of the glass on which isolated laminins were plated in the AFM experiments is likely to override any laminin-specific effects. It is therefore likely that biochemical signals derived from endothelial adhesion to laminin 511 act downstream to regulate actin arrangements and thereby cortical stiffness and mechanotransduction processes (Hutcheson & Griffith, 1996; Tzima *et al*, 2001). Candidate downstream signalling molecules include RhoA, which has been implicated in force generation via $\beta 1$ -integrins (Schiller *et al*, 2013) and shear responses (Jalali *et al*, 1998; Tzima *et al*, 2001), and Src kinase (Huvneers & Danen, 2009; Martinez-Rico *et al*, 2010).

In conclusion, our interdisciplinary approach, combining physiological, biochemical and biophysical analyses of resistance arteries, supports a central role for the endothelial cell basement membrane protein laminin 511 in *in vivo* endothelial cell shear stress mechanotransduction and identify two potential mechanisms of action—remodelling of integrin $\beta 1$ -containing adhesion complexes and stabilization of VE-cadherin at cell-to-cell junctions (Fig 8). Our data suggest that laminin 511 interactions are required for maintaining a healthy responsive endothelium in resistance arteries.

Materials and Methods

Mice and cells

The laminin $\alpha 4$ (*Lama4*^{-/-}) (Thyboll *et al*, 2002) and endothelial cell-specific laminin $\alpha 5$ knockout mouse (*Tek-Cre::Lama5*^{-/-}; Song *et al*, 2013) have been previously described. The Tie2 promoter drives Cre recombinase expression in the *Tek-Cre::Lama5*^{-/-} mice and is active in all endothelial cells by E9.5 (Kisanuki *et al*, 2001) prior to any *Lama5* endothelial expression (Sorokin *et al*, 1997). All experiments were conducted according to German and Swedish Animal Welfare guidelines.

Human umbilical artery endothelial cells (HUAECs), obtained from Promo Cell, were cultured in endothelial cell growth medium (Promo Cell) at 37°C and 5% CO₂ and employed up to passage 8. Mouse skin-derived endothelial cell line (sEND.1) was immortalized using the polyoma middle T oncogene (Williams *et al*, 1989), which was grown in Dulbecco's MEM (DMEM/high glucose) plus 10% FCS, at 37°C and 7.5% CO₂. Authentication of HUAECs and sEND.1 was according to the recommendations of ATCC; cells were tested

for expression of endothelial markers including LDL uptake and PECAM-1, and E-selectin in the case of sEND.1. sEND.1 was tested regularly for maintenance of expression of these endothelial markers. HUAECs were tested for the absence of HIV-1, HIV-2, HBV, HCV and microbial contaminants, including mycoplasma; sEND.1 cells were tested regularly for the absence of mycoplasma by PCR (van Kuppeveld *et al*, 1994) and by staining with Hoechst dye (Chen, 1977).

Immunofluorescence staining and adhesion complexes quantification

Immunofluorescence staining was performed on 5- μ m cryosections as previously described (Sixt *et al*, 2001a). For whole-mount staining of mesenteric resistance arteries, mice were perfused i.v. with 4% ice-cold paraformaldehyde (PFA) and the whole intestine was excised. Dissected resistance arteries were post-fixed at 4°C in 1% PFA in phosphate-buffered saline (PBS) containing 0.1% triethanolamine, 0.1% Triton X-100, 0.1% Nonidet[®] P-40. Arteries were opened longitudinally and incubated in 1% bovine serum albumin (BSA) in PBS containing 1% Triton X-100, followed by overnight staining with primary antibody diluted in 1% BSA, 0.3% Triton X-100 in PBS. Secondary antibodies were diluted in PBS containing 1 μ g/ml DAPI and 0.3% Triton X-100 and incubated for 1 h with the arteries. For cell staining, HUAECs were grown on coated glass coverslips, fixed with ice-cold 1% PFA in PBS and stained as previously described (Sixt *et al*, 2001a). Samples were analysed using a Zeiss AxioImager equipped with epifluorescent optics or a Zeiss LSM 700 confocal microscope. Images were analysed using Volocity 5.5 software (Perkin Elmer). Vinculin-positive adhesion complexes were quantified using maximum intensity projections of each acquired image. Single cells were manually identified as “region of interest,” and adhesion complexes were quantified with ImageJ software.

Antibodies and proteins

The following antibodies were employed in immunofluorescence and *in vitro* assays, unless otherwise stated: rabbit antibodies to mouse laminin $\alpha 4$ (377) (Ringelmann *et al*, 1999), laminin $\alpha 5$ (405) (Ringelmann *et al*, 1999); laminin $\alpha 1$ (317) (Durbeej *et al*, 1996), laminin $\alpha 2$ (401) (Ringelmann *et al*, 1999), laminin $\beta 1$ (Sasaki *et al*, 2002), laminin $\beta 2$ (Sasaki *et al*, 2002), laminin $\gamma 3$ (Gersdorff *et al*, 2005), collagen type IV (AB756P, Millipore), nidogen 1 (Fox *et al*, 1991), nidogen 2 (Kohfeldt *et al*, 1998), perlecan (Costell *et al*, 1997); rat anti-mouse laminin $\gamma 1$ (3E10) (Sixt *et al*, 2001b), PECAM-1 (MEC13.3, BD Bioscience), laminin $\alpha 5$ (4G6) (Sorokin *et al*, 1997), integrin $\beta 1$ (9EG7) (Lenter *et al*, 1993), phospho-myosin light chain 2 (3671, Cell Signaling), vinculin (AB73412, Abcam); goat anti-human VE-cadherin (C-19, Santa Cruz); mouse anti-alpha-smooth muscle actin (C6198, Sigma), rabbit anti-cyclooxygenase2 (Cox2) (4842, Cell Signaling). Secondary antibodies employed were the following: Cy3 donkey anti-rat (712-166-153, Dianova/Jackson Immunoresearch), AF647 donkey anti-rat (AB150155, Abcam), AF488 goat anti-rabbit (A-11008, Molecular Probes/Invitrogen), AF647 goat anti-rabbit (111-605-144, Dianova/Jackson Immunoresearch), AF594 donkey anti-rabbit (A21207, Invitrogen), AF488 donkey anti-goat (A11055, Molecular Probes/Invitrogen), HRP goat

anti-rabbit (172-1019, Bio-Rad). AF488-phalloidin (Life Technologies, A12379) was employed for F-actin staining.

For adhesion assays, the following function-blocking antibodies were employed: rat anti-integrin $\alpha 6$ (GoH3) (Sonnenberg *et al*, 1987) and mouse anti-human integrin $\beta 1$ (P5D2) (Wayner & Carter, 1987), integrin $\alpha 3$ (P1B5) (Wayner & Carter, 1987), integrin $\alpha 5$ (P1D6) (Wayner & Carter, 1987) and integrin αv (LM609) (Mitjans *et al*, 1995).

Laminins 111, 411 and 511 were purified as previously described (Sixt *et al*, 2001b). Fibronectin was purified from human serum (Vuento & Vaheri, 1979).

Scanning electron microscopy of endothelium-denuded arteries

Mesenteric resistance arteries were dissected, open longitudinally and denuded from endothelium by incubation in 50 mM Tris-HCl plus 20 mM EDTA, pH 7.4, plus proteinase inhibitors (Roche), followed by a second incubation in 50 mM Tris-HCl, 1 M NaCl, pH 7.4, plus proteinase inhibitors. Arteries were then processed for electron microscopy as described (Maser & Trimble, 1977). Samples were visualized and imaged with a Hitachi FESEM S5000, 20 kV.

Pressure myograph analyses

WT, *Lam $\alpha 4^{-/-}$* and *Tek-Cre::Lama5 $^{-/-}$* mice were euthanized by cervical dislocation; second-/third-order small mesenteric arteries were cleaned from surrounding tissues and 4- to 5-mm vessel segments were mounted on glass cannulas ($\approx 90 \mu\text{m}$ tip diameter) in a heated pressure myograph chamber (Living Systems Instrumentation, Burlington, VT, USA).

Mesenteric resistance arteries in Ca^{2+} -free HEPES-buffered Krebs solution were mounted on glass cannulae in a pressure myograph chamber (Living Systems Instrumentation, Burlington, VT). Vessels were equilibrated in HEPES-buffered Krebs solution (composed of 135.5 mM NaCl, 5.9 mM KCl, 2.5 mM CaCl_2 , 1.2 mM MgCl_2 , 11.6 mM glucose, and 11.6 mM HEPES, pH 7.4) at 45 mmHg and 38°C and monitored continuously in real time using a Nikon Diaphot 200 inverted microscope equipped with a CCD camera. VediView 1.2 software (Danish MyoTechnology) was used to determine vessel diameter. Flow-induced dilation, myogenic response and passive diameter/pressure relationships were analysed: during the 30 min of equilibration period, 0.3 μM phenylephrine (Sigma-Aldrich) was added to the vessel lumen at a speed of 0.1 $\mu\text{l}/\text{min}$ (shear stress was calculated before running the pump to keep it at less than 10 dynes/cm² to preserve endothelial cell integrity). At the end of the equilibration period, the pressure was increased to 70 mmHg for 5 min before stabilizing at 95 mmHg. To maintain stable vessel tone, 0.3 μM phenylephrine was also added to the bath in which the vessel was suspended. Shear stress rate was calculated using the formula: $\tau = 4\mu Q/\pi r^3$, where μ is viscosity (0.007 poise), Q is the flow (cm³/s) and r is the vessel radius (cm). Vessels were stepwise subjected to 2, 2.5, 5, 10, 20 and 40 dynes/cm², maintaining the direction of shear as originally in the animal. The shear level was maintained for 2 min, and vessel diameter was then measured. At the end of every flow-induced dilation experiment, endothelial cell viability was checked by adding 10 μM (final concentration) acetylcholine (ACh) (Sigma-Aldrich). Unresponsive vessels were excluded from final analyses. For the myogenic response,

intraluminal pressure was set at 20, 45, 70, 95 and 120 mmHg. Each pressure level was maintained for 5 min, and the vessel diameter was measured. Myogenic tone at each pressure was calculated as: myogenic tone = $(D_p - D_a)/D_p \times 100$, where D_p is the passive vessel diameter measured after every experiment in Ca^{2+} -free HEPES-buffered Krebs solution plus 2 mM EGTA, and D_a is the active diameter, that is, the diameter calculated during the myogenic response.

Wire myograph analyses

Mesenteric resistance arteries were collected in ice-cold 3-N-morpholino propane sulphonic acid (MOPS) buffer and mounted on the wire myograph. After exchanging the buffer with physiological saline solution containing 5 mM HEPES (PSS) (gassed with 5% CO₂, pH 7.4), vessels were normalized to the diameter that they would have *in situ* when relaxed and under a transmural pressure of 100 mmHg (Mulvany & Halpern, 1977). Vessel viability was checked by replacing PSS with PSS containing potassium (KPSS) for 5 min, vessels that did not show any force development were discarded. After several washes to allow vessels to reach baseline force levels, responses to different doses of contractile drugs (U46619, phenylephrine) were measured, or the vessels were pre-constricted with a submaximal dose of U46119 (3×10^{-7} M) and the effects of vasodilatory drugs (sodium nitroprusside, methacholine) were tested.

Atomic force microscopy

AFM was employed to measure cortical stiffness as previously described (Oberleithner *et al*, 2009). Briefly, the measurements consisted of gradually approaching a non-coated polystyrene spherical cantilever tip (10 μm diameter; Novascan) onto the endothelial cell for approximately 200 nm in order to record its cortical stiffness (50–150 nm depth). For endothelial cell measurements, sEND.1 (Williams *et al*, 1989) or HUAECs were seeded onto glass coverslips coated with different concentrations of purified laminin 511, laminin 411 or laminin 111 (1, 5, 10, 20 and 30 nM). At least two coverslips were employed for each laminin concentration tested. Aortas were collected and cleaned from the surrounding adipose tissue, and equal-sized rings were obtained from each vessel. The aortic rings were opened longitudinally to expose the endothelium, stuck onto a 15-mm-diameter glass coverslips using Cell-Tak™ (BD Bioscience) and kept at 37°C and 5% CO₂ in DMEM (Invitrogen) until the AFM measurement. The quality of the aortic endothelial cell layer was checked after AFM by immunofluorescence staining for endothelial cell markers, such as PECAM-1 or VE-cadherin. Control experiments were performed with mesenteric resistance arteries. The force–distance curves obtained from the AFM measurements were analysed with the protein unfolding and nano-indentation analysis software PUNIAS version 1.0, release 1.8 to calculate cortical stiffness of the endothelial cells.

Adhesion assay

Cell adhesion assays were performed with HUAECs and mouse sEND.1 cells as previously described (Sixt *et al*, 2001b). Substrates employed included the endothelial laminins 411 and 511, non-endothelial laminin 111 and fibronectin. Cells were incubated for

45 min at 37°C, and bound cells were measured using the hexosaminidase assay (Landegren, 1984) or violet blue staining of cells and manual counting. Inhibition assays to determine receptors required for binding to the different ECM substrates involved a 10- to 15-min pre-incubation of cells on ice with 15–20 $\mu\text{g}/\text{ml}$ blocking antibody, prior to adding cells and antibody to the substrates. Only saturating concentrations of the laminin isoforms were employed (20–30 $\mu\text{g}/\text{ml}$) and adhesion was measured at times points when adhesion to the substrate had plateaued (1–2 h). Functional-blocking antibodies to human integrins $\beta 1$ (P5D2), $\alpha 3$ (P1B5), $\alpha 6$ (GoH3), $\alpha 5$ (P1D6) and $\alpha \nu$ (LM609) were employed either alone or in combination.

Dual pipette assay

To determine whether cell–cell adhesion strengths were affected by endothelial cell adhesion to different laminins, a dual pipette assay was performed (Chu *et al*, 2004; Martinez-Rico *et al*, 2010). Polystyrene macrobeads (15 μm , Polysciences, Inc.) were coated overnight at 4°C with 20 μM purified laminin 511, laminin 411 or laminin 111, added to a cell suspension of HUAECs in HEPES-buffered cell culture medium at a ratio of 1:2 and incubated at 37°C, 5% CO_2 for 1 h to permit cell adhesion to the coated beads. Individual cells bound to a bead were captured using micropipettes connected to a micromanipulator and a hydraulic-pneumatic system with a pressure sensor. Two cells were permitted to bind to each other for 5 min, after which one cell was fixed by one micropipette, while the other was pulled away by stepwise increases in aspiration force. The aspiration forces prior to detachment of the two cells (P_{n-1}) and at the time point of detachment (P_n) were recorded, and the adhesion strength (AS) was calculated: $AS = \pi(d/2)^2 (P_{n-1} + P_n)/2$, where d is the inner diameter of the pipette. Controls included the addition of VE-cadherin-blocking antibody (BV9, Santa Cruz), integrin $\beta 1$ -blocking antibody (P5D2) or IgG_{2a} isotope control (Santa Cruz) diluted in the HEPES-buffered cell culture medium and added to dissociated cells directly before the measurements. To some experiments, 10 μM ROCK inhibitor Y27632 (Y0503, SIGMA), focal adhesion kinase inhibitor I (324877, MERK-Millipore) or SRC inhibitor PP1 (567809, MERK-Millipore) was added to the HEPES-buffered medium containing cell–bead complexes 10 min before measurements were taken.

To investigate whether laminin 511 effects were due to the strength of HUAEC adhesion to this substrate, experiments were also performed using soluble laminin 511 (20 μM) added to the medium, individual cells were then captured directly by micropipettes and the strength of cell–cell adhesion was measured as above, in the presence or absence of anti-VE-cadherin or anti-integrin $\beta 1$ antibody.

Antibody-feeding assay

To determine junctional levels of VE-cadherin, HUAECs were seeded onto glass coverslips coated with 20 nM purified laminin 511, laminin 411 or laminin 111. After 6 h in culture, the confluent cell layer was incubated for 30 min with 2.5 $\mu\text{g}/\text{ml}$ mouse anti-human VE-cadherin (BV9, Abcam). Cells were washed and fixed with 4% PFA, and surface-bound anti-VE-cadherin was bound with excess

Alexa 488-conjugated donkey anti-mouse antibody. Cells were then permeabilized with 0.2% Triton X-100 in PBS, post-fixed with 4% PFA and incubated with Cy3-conjugated goat anti-mouse antibody to detect internalized anti-VE-cadherin. Cells were examined using a Zeiss LSM 700, and numbers of Cy3-positive vesicles containing internalized VE-cadherin were determined using Volocity5.5 software.

Surface biotinylation assay and Western blot

To determine surface levels of VE-cadherin, HUAECs were seeded at confluency in 6-cm Petri dishes coated with 20 μM purified laminin 511, laminin 411 or laminin 111. Cells were subsequently incubated with 4 mM EGTA for 20 min and then moved to 4°C and incubated with 0.5 mg/ml sulfo-NHS-biotin (Life Technologies) for 1 h. After quenching unbound biotin with ice-cold 100 mM glycine in PBS, total proteins were extracted in the presence of proteinase inhibitor cocktail (Roche) and the biotinylated proteins were precipitated with NeutrAvidin™ agarose beads (Life Technologies). The amount of VE-cadherin in the precipitated biotinylated proteins (surface bound) and the total VE-cadherin protein (input) in the sample before immunoprecipitation of biotinylated proteins were analysed by fluorescence Western blotting (Gingrich *et al*, 2000) using a polyclonal goat anti-human VE-cadherin antibody (C-19, Santa Cruz). The blots were quantified using the gel analysis functionality of the software ImageJ; the precipitate results were normalized to total protein (<http://rsb.info.nih.gov/ij/docs/menus/analyze.html#gels>).

VE-cadherin co-immunoprecipitation

HUAECs were plated at confluent density on 20 nM purified laminin 511 and 111. After 6 h in culture, the total proteins were extracted and VE-cadherin was precipitated with anti-human polyclonal antibody (C-19) conjugated to protein G–Sepharose beads (GE Healthcare). The amount of coprecipitated p120 catenin was quantified by fluorescence Western Blots using a rabbit anti-human p120 catenin antibody (S-19, Santa Cruz). Normal goat IgG (Santa Cruz) was used as isotope control in the precipitation process.

Intravital microscopy of mesenteric arteries

To determine the average size of mesenteric arteries *in vivo* WT, *Lama4*^{-/-} and *Tek-Cre::Lama5*^{-/-} mice were anaesthetized using intraperitoneal (i.p.) injection of a mixture of ketamine hydrochloride (125 mg/kg) and xylazine (12.5 mg/kg) in saline. The distal tract of small intestine was exposed, and first-order mesenteric arteries were imaged using a Zeiss AxioScope A1 microscope equipped with a saline immersion objective (SW 40/0.75 NA) and stroboscopic epifluorescent illumination (Colibri-2, Zeiss). The animal temperature was kept at 37°C with a heat pad. Autofluorescence of the internal elastic lamina as shown in Fig 2C was employed as an approximate marker of the inner lining of arteries and for measures of vessel diameters.

Arterial blood pressure measurement

Mean systolic and diastolic blood pressures were measured in WT, *Lama4*^{-/-} and *Tek-Cre::Lama5*^{-/-} mice anaesthetized using

isoflurane–air mixture; their body temperature was kept constant with a heating pad. The right common carotid was exposed, and a 25G Millar catheter connected to pressure transducer was inserted approximately 9 mm into the vessel to reach the aortic arch, and the blood pressure was recorded for 10 min.

Shear stress-induced COX2 expression and HUAEC alignment

HUAECs were plated at confluent density on 25 nM purified laminin 511 and 111 in chamber slides (μ -Slide I^{0.2} Luer or μ -Slide VI^{0.4}; Ibidi) and then subjected to 10 dyn/cm² or no shear for 4 h using an Ibidi pump system. Control cells (static) and shear-subjected cells were collected, and mRNA was extracted using an RNeasy Mini Kit (Qiagen). Quantitative real-time PCR was performed with 10 ng amplified cDNA per sample in an Rotor-Gene Q (Qiagen) using Brilliant SYBR Green QPCR Master Mix (Agilent Technologies). Results were normalized to Top1 expression levels. The following primers sequences were employed:

Cox2 – Fwd 5' AAGTGGCATTGTACCCGGAC 3';
Rev 5' TTTGTAGCCATAGTCAGCATTGT 3';
Top1 – Fwd 5' CCAACGGAAGCTCGGAAAC 3';
Rev R 5' GTCCAGGAGGCTCTATCTTAA 3'.

Total proteins were extracted from control (static) and shear-subjected HUAECs, and the COX2 protein levels were detected by Western blots. Quantification of band intensities was performed with ImageJ software.

To quantify HUAEC orientation in response to shear stress, live imaging was performed over 120 min using the conditions described above. Cell alignment was documented using a Zeiss Axiovert 200M equipped with a temperature and CO₂ controller. Cell orientation was analysed first with *FogBank* technique (Chalfoun *et al*, 2014) and quantified using ImageJ software.

Expanded View for this article is available online.

Acknowledgements

This work was supported by the Marie Curie Initial Training Networks, SmArt and SmArtER, the Swedish Research Council, the Swedish Heart and Lung Foundation and by funding from the German Research Foundation to LS (CRC 1009 A02) and to JDR (EXE 1003, CiM Bridging Fellowship). We thank Bernhard Nieswandt, University of Würzburg, for the generous gift of anti-mouse integrin $\beta 3$ antibody and Erez Raz for help with the dual pipette assays.

Author contributions

JDR carried out most experiments and was involved in designing some experiments; A-LL carried out cell adhesion assays, VE-cadherin recycling studies and shear stress analyses; LY tested smooth muscle contraction and dilation in the *Lama4*^{-/-} mice; SB produced and tested all laminins; HO and VH performed AFM experiments; JK aided in the electron microscopy analyses; EVB and ENTPB aided in wire myograph studies; PH, AB and SA aided in the shear experiments; FP aided in dual pipette assays; RH and LMS designed experiments; LMS supervised all work; and LMS and JDR wrote the manuscript.

Conflict of interest

The authors declare that they have no conflict of interest.

References

- Abraham S, Yeo M, Montero-Balaguer M, Paterson H, Dejana E, Marshall CJ, Mavria G (2009) VE-Cadherin-mediated cell-cell interaction suppresses sprouting via signaling to MLC2 phosphorylation. *Curr Biol* 19: 668–674
- Albinsson S, Shakirova Y, Rippe A, Baumgarten M, Rosengren BI, Rippe C, Hallmann R, Hellstrand P, Rippe B, Sward K (2007) Arterial remodeling and plasma volume expansion in caveolin-1-deficient mice. *Am J Physiol Regul Integr Comp Physiol* 293: R1222–R1231
- Belin de Chantemele EJ, Vessieres E, Guihot AL, Toutain B, Maquignau M, Loufrani L, Henrion D (2009) Type 2 diabetes severely impairs structural and functional adaptation of rat resistance arteries to chronic changes in blood flow. *Cardiovasc Res* 81: 788–796
- Bogdani M, Korpos E, Simeonovic CJ, Parish CR, Sorokin L, Wight TN (2014) Extracellular matrix components in the pathogenesis of type 1 diabetes. *Curr Diab Rep* 14: 552
- Bouvet C, Belin de Chantemele E, Guihot AL, Vessieres E, Bocquet A, Dumont O, Jardel A, Loufrani L, Moreau P, Henrion D (2007) Flow-induced remodeling in resistance arteries from obese Zucker rats is associated with endothelial dysfunction. *Hypertension* 50: 248–254
- Brevier J, Vallade M, Riveline D (2007) Force-extension relationship of cell-cell contacts. *Phys Rev Lett* 98: 268101
- Chalfoun J, Majurski M, Dima A, Stuelten C, Peskin A, Brady M (2014) FogBank: a single cell segmentation across multiple cell lines and image modalities. *BMC Bioinformatics* 15: 431
- Chen TR (1977) *In situ* detection of mycoplasma contamination in cell cultures by fluorescent Hoechst 33258 stain. *Exp Cell Res* 104: 255–262
- Chiasson CM, Wittich KB, Vincent PA, Faundez V, Kowalczyk AP (2009) p120-catenin inhibits VE-cadherin internalization through a Rho-independent mechanism. *Mol Biol Cell* 20: 1970–1980
- Chiu YJ, McBeath E, Fujiwara K (2008) Mechanotransduction in an extracted cell model: Fyn drives stretch- and flow-elicited PECAM-1 phosphorylation. *J Cell Biol* 182: 753–763
- Chu YS, Thomas WA, Eder O, Pincet F, Perez E, Thiery JP, Dufour S (2004) Force measurements in E-cadherin-mediated cell doublets reveal rapid adhesion strengthened by actin cytoskeleton remodeling through Rac and Cdc42. *J Cell Biol* 167: 1183–1194
- Collins C, Osborne LD, Guilluy C, Chen Z, O'Brien ET III, Reader JS, Burrige K, Superfine R, Tzima E (2014) Haemodynamic and extracellular matrix cues regulate the mechanical phenotype and stiffness of aortic endothelial cells. *Nat Commun* 5: 3984
- Conway DE, Breckenridge MT, Hinde E, Gratton E, Chen CS, Schwartz MA (2013) Fluid shear stress on endothelial cells modulates mechanical tension across VE-Cadherin and PECAM-1. *Curr Biol* 23: 1024–1030
- Coon BG, Baeyens N, Han J, Budatha M, Ross TD, Fang JS, Yun S, Thomas JL, Schwartz MA (2015) Intramembrane binding of VE-cadherin to VEGFR2 and VEGFR3 assembles the endothelial mechanosensory complex. *J Cell Biol* 208: 975–986
- Costell M, Mann K, Yamada Y, Timpl R (1997) Characterization of recombinant perlecan domain I and its substitution by glycosaminoglycans and oligosaccharides. *Eur J Biochem* 243: 115–121
- Daneshjoui N, Sieracki N, van Nieuw Amerongen GP, Schwartz MA, Komarova YA, Malik AB, Conway DE (2015) Rac1 functions as a reversible tension modulator to stabilize VE-cadherin trans-interaction. *J Cell Biol* 208: 23–32

- Davies PF, Robotewskij A, Griem ML (1994) Quantitative studies of endothelial cell adhesion. Directional remodeling of focal adhesion sites in response to flow forces. *J Clin Invest* 93: 2031–2038
- Discher DE, Janmey P, Wang YL (2005) Tissue cells feel and respond to the stiffness of their substrate. *Science* 310: 1139–1143
- Dumont O, Kauffenstein G, Guihot AL, Guerineau NC, Abraham P, Loufrani L, Henrion D (2014) Time-related alteration in flow- (shear stress-) mediated remodeling in resistance arteries from spontaneously hypertensive rats. *Int J Hypertens* 2014: 859793
- Durbeej M, Fecker L, Hjalt T, Zhang HY, Salmivirta K, Klein G, Timpl R, Sorokin L, Ebdal T, Ekblom P, Ekblom M (1996) Expression of laminin alpha 1, alpha 5 and beta 2 chains during embryogenesis of the kidney and vasculature. *Matrix Biol* 15: 397–413
- Engl W, Arasi B, Yap LL, Thiery JP, Viasnoff V (2014) Actin dynamics modulate mechanosensitive immobilization of E-cadherin at adherens junctions. *Nat Cell Biol* 16: 587–594
- Fleming I, Fisslthaler B, Dixit M, Busse R (2005) Role of PECAM-1 in the shear-stress-induced activation of Akt and the endothelial nitric oxide synthase (eNOS) in endothelial cells. *J Cell Sci* 118: 4103–4111
- van der Flier A, Badu-Nkansah K, Whittaker CA, Crowley D, Bronson RT, Lacy-Hulbert A, Hynes RO (2010) Endothelial alpha5 and alpha v integrins cooperate in remodeling of the vasculature during development. *Development* 137: 2439–2449
- Fox JW, Mayer U, Nischt R, Aumailley M, Reinhardt D, Wiedemann H, Mann K, Timpl R, Krieg T, Engel J, Chu M-L (1991) Recombinant nidogen consists of three globular domains and mediates binding of laminin to collagen type IV. *EMBO J* 10: 3136–3146
- Frangos JA, Eskin SG, McIntire LV, Ives CL (1985) Flow effects on prostacyclin production by cultured human endothelial cells. *Science* 227: 1477–1479
- Fujiwara H, Kikkawa Y, Sanzen N, Sekiguchi K (2001) Purification and characterization of human laminin-8. Laminin-8 stimulates cell adhesion and migration through alpha3beta1 and alpha6beta1 integrins. *J Biol Chem* 276: 17550–17558
- van Geemen D, Smeets MW, van Stalborch AM, Woerdeman LA, Daemen MJ, Hordijk PL, Huveneers S (2014) F-actin-anchored focal adhesions distinguish endothelial phenotypes of human arteries and veins. *Arterioscler Thromb Vasc Biol* 34: 2059–2067
- Geiger B, Spatz JP, Bershadsky AD (2009) Environmental sensing through focal adhesions. *Nat Rev Mol Cell Biol* 10: 21–33
- Gersdorff N, Kohfeldt E, Sasaki T, Timpl R, Miosge N (2005) Laminin gamma3 chain binds to nidogen and is located in murine basement membranes. *J Biol Chem* 280: 22146–22153
- Gingrich JC, Davis DR, Nguyen Q (2000) Multiplex detection and quantitation of proteins on western blots using fluorescent probes. *Biotechniques* 29: 636–642
- Hahn C, Schwartz MA (2009) Mechanotransduction in vascular physiology and atherogenesis. *Nat Rev Mol Cell Biol* 10: 53–62
- Halder G, Dupont S, Piccolo S (2012) Transduction of mechanical and cytoskeletal cues by YAP and TAZ. *Nat Rev Mol Cell Biol* 13: 591–600
- Hallmann R, Horn N, Selg M, Wendler O, Pausch F, Sorokin LM (2005) Expression and function of laminins in the embryonic and mature vasculature. *Physiol Rev* 85: 979–1000
- Hutcheson IR, Griffith TM (1996) Mechanotransduction through the endothelial cytoskeleton: mediation of flow- but not agonist-induced EDRF release. *Br J Pharmacol* 118: 720–726
- Huveneers S, Danen EH (2009) Adhesion signaling – crosstalk between integrins, Src and Rho. *J Cell Sci* 122: 1059–1069
- Ingber DE, Jamieson JD (1985) Cells as tensegrity structures: architectural regulation of histodifferentiation by physical forces over basement membranes. In *Gene expression during normal and malignant differentiation*, Andersson CG, Gahmberg LC, Ekblom P (eds), pp 13–32. London: Academic Press
- Intengan HD, Schiffrin EL (2000) Structure and mechanical properties of resistance arteries in hypertension: role of adhesion molecules and extracellular matrix determinants. *Hypertension* 36: 312–318
- Jalali S, Li YS, Sotoudeh M, Yuan S, Li S, Chien S, Shyy JY (1998) Shear stress activates p60src-Ras-MAPK signaling pathways in vascular endothelial cells. *Arterioscler Thromb Vasc Biol* 18: 227–234
- Jalali S, del Pozo MA, Chen K, Miao H, Li Y, Schwartz MA, Shyy JY, Chien S (2001) Integrin-mediated mechanotransduction requires its dynamic interaction with specific extracellular matrix (ECM) ligands. *Proc Natl Acad Sci USA* 98: 1042–1046
- Jin ZG, Ueba H, Tanimoto T, Lungu AO, Frame MD, Berk BC (2003) Ligand-independent activation of vascular endothelial growth factor receptor 2 by fluid shear stress regulates activation of endothelial nitric oxide synthase. *Circ Res* 93: 354–363
- Kikkawa Y, Sanzen N, Fujiwara H, Sonnenberg A, Sekiguchi K (2000) Integrin binding specificity of laminin-10/11: laminin-10/11 are recognized by alpha 3 beta 1, alpha 6 beta 1 and alpha 6 beta 4 integrins. *J Cell Sci* 113 (Pt 5): 869–876
- Kisanuki YY, Hammer RE, Miyazaki J, Williams SC, Richardson JA, Yanagisawa M (2001) Tie2-Cre transgenic mice: a new model for endothelial cell-lineage analysis *in vivo*. *Dev Biol* 230: 230–242
- Kohfeldt E, Sasaki T, Gohring W, Timpl R (1998) Nidogen-2: a new basement membrane protein with diverse binding properties. *J Mol Biol* 282: 99–109
- van Kuppeveld FJ, Johansson KE, Galama JM, Kissing J, Bolske G, van der Logt JT, Melchers WJ (1994) Detection of mycoplasma contamination in cell cultures by a mycoplasma group-specific PCR. *Appl Environ Microbiol* 60: 149–152
- Landegren U (1984) Measurement of cell numbers by means of the endogenous enzyme hexosaminidase. Applications to detection of lymphokines and cell surface antigens. *J Immunol Methods* 67: 379–388
- Lenter M, Uhlig H, Hamann A, Jenö P, Imhof B, Vestweber D (1993) A monoclonal antibody against an activation epitope on mouse integrin chain beta 1 blocks adhesion of lymphocytes to the endothelial integrin alpha 6 beta 1. *Proc Natl Acad Sci USA* 90: 9051–9055
- Levesque MJ, Nerem RM (1985) The elongation and orientation of cultured endothelial cells in response to shear stress. *J Biomech Eng* 107: 341–347
- Liu Z, Tan JL, Cohen DM, Yang MT, Sniadecki NJ, Ruiz SA, Nelson CM, Chen CS (2010) Mechanical tugging force regulates the size of cell-cell junctions. *Proc Natl Acad Sci USA* 107: 9944–9949
- Martinez-Rico C, Pincet F, Thiery JP, Dufour S (2010) Integrins stimulate E-cadherin-mediated intercellular adhesion by regulating Src-kinase activation and actomyosin contractility. *J Cell Sci* 123: 712–722
- Maser MD, Trimble JJ III (1977) Rapid chemical dehydration of biologic samples for scanning electron microscopy using 2,2-dimethoxypropane. *J Histochem Cytochem* 25: 247–251
- Matrougui K, Schiavi P, Guez D, Henrion D (1998) High sodium intake decreases pressure-induced (myogenic) tone and flow-induced dilation in resistance arteries from hypertensive rats. *Hypertension* 32: 176–179
- Mitjans F, Sander D, Adan J, Sutter A, Martinez JM, Jaggel CS, Moyano JM, Kreysch HG, Piulats J, Goodman SL (1995) An anti-alpha v-integrin

- antibody that blocks integrin function inhibits the development of a human melanoma in nude mice. *J Cell Sci* 108(Pt 8): 2825–2838
- Mulvany MJ, Halpern W (1977) Contractile properties of small arterial resistance vessels in spontaneously hypertensive and normotensive rats. *Circ Res* 41: 19–26
- Mulvany MJ (1999) Vascular remodelling of resistance vessels: can we define this? *Cardiovasc Res* 41: 9–13
- Nielsen PK, Yamada Y (2001) Identification of cell-binding sites on the Laminin alpha 5 N-terminal domain by site-directed mutagenesis. *J Biol Chem* 276: 10906–10912
- van Nieuw Amerongen GP, Beckers CM, Achekar ID, Zeeman S, Musters RJ, van Hinsbergh VW (2007) Involvement of Rho kinase in endothelial barrier maintenance. *Arterioscler Thromb Vac Biol* 27: 2332–2339
- Oberleithner H, Callies C, Kusche-Vihrog K, Schillers H, Shahin V, Riethmuller C, Macgregor GA, de Wardener HE (2009) Potassium softens vascular endothelium and increases nitric oxide release. *Proc Natl Acad Sci USA* 106: 2829–2834
- Orr AW, Ginsberg MH, Shattil SJ, Deckmyn H, Schwartz MA (2006) Matrix-specific suppression of integrin activation in shear stress signaling. *Mol Biol Cell* 17: 4686–4697
- Rauch U, Saxena A, Lorkowski S, Rauterberg J, Bjorkbacka H, Durbeek J, Hultgardh-Nilsson A (2011) Laminin isoforms in atherosclerotic arteries from mice and man. *Histol Histopathol* 26: 711–724
- Ringelmann B, Roder C, Hallmann R, Maley M, Davies M, Grounds M, Sorokin L (1999) Expression of laminin alpha1, alpha2, alpha4, and alpha5 chains, fibronectin, and tenascin-C in skeletal muscle of dystrophic 129Rej dy/dy mice. *Exp Cell Res* 246: 165–182
- Riveline D, Zamir E, Balaban NQ, Schwarz US, Ishizaki T, Narumiya S, Kam Z, Geiger B, Bershadsky AD (2001) Focal contacts as mechanosensors: externally applied local mechanical force induces growth of focal contacts by an mDia1-dependent and ROCK-independent mechanism. *J Cell Biol* 153: 1175–1186
- Sasaki T, Timpl R (2001) Domain IVa of laminin alpha5 chain is cell-adhesive and binds beta1 and alphaVbeta3 integrins through Arg-Gly-Asp. *FEBS Lett* 509: 181–185
- Sasaki T, Mann K, Miner JH, Miosge N, Timpl R (2002) Domain IV of mouse laminin beta1 and beta2 chains. *Eur J Biochem* 269: 431–442
- Sauteur L, Krudewig A, Herwig L, Ehrenfeuchter N, Lenard A, Affolter M, Belting HG (2014) Cdh5/VE-cadherin promotes endothelial cell interface elongation via cortical actin polymerization during angiogenic sprouting. *Cell Rep* 9: 504–513
- Schiller HB, Hermann MR, Polleux J, Vignaud T, Zanivan S, Friedel CC, Sun Z, Raducanu A, Gottschalk KE, Thery M, Mann M, Fassler R (2013) beta1- and alphaV-class integrins cooperate to regulate myosin II during rigidity sensing of fibronectin-based microenvironments. *Nat Cell Biol* 15: 625–636
- Sixt M, Engelhardt B, Pausch F, Hallmann R, Wendler O, Sorokin LM (2001a) Endothelial cell laminin isoforms, laminin 8 and 10, play decisive roles in T-cell recruitment across the blood-brain-barrier in an experimental autoimmune encephalitis model (EAE). *J Cell Biol* 153: 933–945
- Sixt M, Hallmann R, Wendler O, Scharffetter-Kochanek K, Sorokin LM (2001b) Cell adhesion and migration properties of b2-integrin negative, polymorphonuclear granulocytes (PMN) on defined extracellular matrix molecules: relevance for leukocyte extravasation. *J Biol Chem* 276: 18878–18887
- Song J, Lokmic Z, Lammernann T, Rolf J, Wu C, Zhang X, Hallmann R, Hannocks MJ, Horn N, Ruegg MA, Sonnenberg A, Georges-Labouesse E, Winkler TH, Kearney JF, Cardell S, Sorokin L (2013) Extracellular matrix of secondary lymphoid organs impacts on B-cell fate and survival. *Proc Natl Acad Sci USA* 110: E2915–E2924
- Sonnenberg A, Janssen H, Hogervorst F, Calafat J, Hilgers J (1987) A complex of platelet glycoproteins Ic and IIa identified by a rat monoclonal antibody. *J Biol Chem* 262: 10376–10383
- Sorokin LM, Pausch F, Frieser M, Kroger S, Ohage E, Deutzmann R (1997) Developmental regulation of the laminin alpha5 chain suggests a role in epithelial and endothelial cell maturation. *Dev Biol* 189: 285–300
- Stenzel D, Franco CA, Estrach S, Mettouchi A, Sauvaget D, Rosewell I, Schertel A, Armer H, Domogatskaya A, Rodin S, Tryggvason K, Collinson L, Sorokin L, Gerhardt H (2011) Endothelial basement membrane limits tip cell formation by inducing Dll4/Notch signalling *in vivo*. *EMBO Rep* 12: 1135–1143
- Thyboll J, Kortessmaa J, Cao R, Soininen R, Wang L, Iivanainen A, Sorokin L, Risling M, Cao Y, Tryggvason K (2002) Deletion of the laminin alpha4 chain leads to impaired microvessel maturation. *Mol Cell Biol* 22: 1194–1202
- Topper JN, Cai J, Falb D, Gimbrone MA Jr (1996) Identification of vascular endothelial genes differentially responsive to fluid mechanical stimuli: cyclooxygenase-2, manganese superoxide dismutase, and endothelial cell nitric oxide synthase are selectively up-regulated by steady laminar shear stress. *Proc Natl Acad Sci USA* 93: 10417–10422
- Tzima E, del Pozo MA, Shattil SJ, Chien S, Schwartz MA (2001) Activation of integrins in endothelial cells by fluid shear stress mediates Rho-dependent cytoskeletal alignment. *EMBO J* 20: 4639–4647
- Tzima E, Irani-Tehrani M, Kiosses WB, Dejana E, Schultz DA, Engelhardt B, Cao G, DeLisser H, Schwartz MA (2005) A mechanosensory complex that mediates the endothelial cell response to fluid shear stress. *Nature* 437: 426–431
- Urbich C, Walter DH, Zeiher AM, Dimmeler S (2000) Laminar shear stress upregulates integrin expression: role in endothelial cell adhesion and apoptosis. *Circ Res* 87: 683–689
- Vessieres E, Freidja ML, Loufrani L, Fassot C, Henrion D (2012) Flow (shear stress)-mediated remodeling of resistance arteries in diabetes. *Vascu Pharmacol* 57: 173–178
- Vuento M, Vaehri A (1979) Purification of fibronectin from human plasma by affinity chromatography under non-denaturing conditions. *Biochem J* 183: 331–337
- Wayner EA, Carter WG (1987) Identification of multiple cell adhesion receptors for collagen and fibronectin in human fibrosarcoma cells possessing unique alpha and common beta subunits. *J Cell Biol* 105: 1873–1884
- Williams RL, Risau W, Zerwer H-G, Drexler H, Aguzzi A, Wagner EF (1989) Endothelioma cells expressing the polyoma middle T oncogene induce hemangiomas by host cell recruitment. *Cell* 57: 1053–1063
- Wu C, Ivars F, Anderson P, Hallmann R, Vestweber D, Nilsson P, Robenek H, Tryggvason K, Song J, Korpos E, Loser K, Beissert S, Georges-Labouesse E, Sorokin LM (2009) Endothelial basement membrane laminin alpha5 selectively inhibits T lymphocyte extravasation into the brain. *Nat Med* 15: 519–527
- Xiao K, Garner J, Buckley KM, Vincent PA, Chiasson CM, Dejana E, Faundez V, Kowalczyk AP (2005) p120-Catenin regulates clathrin-dependent endocytosis of VE-cadherin. *Mol Biol Cell* 16: 5141–5151
- Yamamoto H, Ehling M, Kato K, Kanai K, van Lessen M, Frye M, Zeuschner D, Nakayama M, Vestweber D, Adams RH (2015) Integrin beta1 controls VE-cadherin localization and blood vessel stability. *Nat Commun* 6: 6429



License: This is an open access article under the terms of the Creative Commons Attribution-NonCommercial-NoDerivs 4.0 License, which permits use and distribution in any medium, provided the original work is properly cited, the use is non-commercial and no modifications or adaptations are made.